Innovative preparations of heterogeneous catalysts for the production of (bio)fuels

Ana Teresa Fialho Batista

Thesis to obtain the Master of Science Degree in

Chemical Engineering

Supervisors:

Doctor Audrey Bonduelle-Skrzypczak

Professor Maria Filipa Gomes Ribeiro

Examination Commitee

Chairperson: Professor Sebastião Manuel Tavares da Silva Alves

Supervisor: Professor Maria Filipa Gomes Ribeiro

Member of the Commitee: Professor Carlos Manuel Faria de Barros Henriques

October 2016

(This page was intentionally left in blank)

Acknowledgements

I thank IFPEN and IST for the opportunity to develop this work.

I would like to thank all the IFP professionals that welcomed me and supported me in my work, namely my supervisors: Audrey Bonduelle and Christophe Vallée, Alexandra Chaumonnot and the technicians who trained me: Emmanuel Rosati, Nathalie Lett, Anne Boffo, Florence Del Toso and Corinne Sagnard.

I thank my supervisor at IST, Professor Filipa Ribeiro, not only for her guidance in this work but also for her support and help through my academic development.

Finally I thank my parents, my brother and Diogo for their support and understanding throughout my academic years and of what is yet to come.

Resumo

Especificações de combustíveis mais exigentes e o uso de crudes de pior qualidade pelos refinadores motivam o desenvolvimento de catalisadores cada vez mais eficientes. Nesse contexto, este trabalho tem como objetivo a preparação e caracterização de catalisadores de hidrotratamento (HDT) usando um método de co-mistura mais simples que os tradicionalmente usados. Quatro catalisadores com 10% MoO_3 (m/m_{cata}) foram preparados por co-mistura convencional de dois percursores de alumina (boehmite) com heptamolibdato e com trióxido de molibdénio mais ácido fosfórico. A calcinação foi eliminada para evitar a sinterização do metal e a formação de óxidos estáveis. Os extrudidos de boehmite, secos apenas, foram caracterizados e o comportamento catalítico foi avaliado através da reacção modelo de hidrogenação do tolueno. Os catalisadores sintetizados tiveram piores resultados catalíticos do que o catalisador de referência, o que se pode atribuir ao suporte ser boehmite e não alumina. Os catalisadores obtidos por co-mistura apresentaram, após sulfuração a 350°C, uma taxa de sulfuração do Mo normal.

Para testar condições de mistura particulares, prepararam-se sete suportes de alumina que foram caracterizados em termos de textura. Utilizando estas condições de mistura e um percursor de Mo específico, obtiveram-se nove catalisadores de Mo e dois catalisadores de Mo dopados com outro metal, preparados por co-mistura, caracterizados e testados na reacção de hidrogenação do tolueno. Um dos catalisadores dopados mostrou a mesma performance que a referencia. Os catalisadores obtidos por co-mistura têm um melhor grau de sulfuração após sulfuração a temperatura ambiente, o que se pensa ter um impacto positivo na promoção da fase MoS_2 a alta temperatura.

Palavras-chave: hidrotratamento, catalisador, co-mistura, molibdénio

Abstract

The tightening of liquid fuels' specifications and the use of lower quality crude oils call for a constant effort to develop more efficient catalysts. In this context, the goal of this work was to prepare hydrotreatment (HDT) catalysts using the simpler and shorter method of co-mixing of the metal precursor with an alumina precursor. Four non-promoted molybdenum catalysts with a metal loading of 10% MoO_3 (w/w_{cata}) were produced by co-mixing of two different alumina precursors (boehmite) with heptamolybdate and molybdenum trioxide plus phosphoric acid. Calcination was skipped to avoid metal sintering and stable oxide formation. Thus the dried boehmite extrudates where characterized and tested for toluene hydrogenation. These samples showed a lower activity than the reference catalyst, which can be attributed mainly to having a boehmite (not alumina) support. The co-mixing catalysts present a classic Mo sulphidation after sulphidation at 350°C.

To test particular mixing conditions, seven trial supports were successfully produced and the textural properties were evaluated. Using these mixing conditions and a specific Mo precursor, nine non-promoted and two promoted HDT catalysts were produced by co-mixing, characterized and tested for toluene hydrogenation. Notably, one of the promoted catalysts showed the same performance as the reference, demonstrating that a catalyst produced by a simpler and less time consuming technique of co-mixing can compete with one prepared by impregnation. The co-mixing catalysts also showed a higher Mo sulphidation degree after sulphidation at room temperature. This is considered to positively impact the promotion of the MoS_2 slabs at higher temperatures.

Key-words: hydrotreatment, catalyst, co-mixing, molybdenum

Table of Contents

List of Figures

List of Tables

Abbreviations List

DTA – differential thermal analysis

EPMA – electron probe microanalyser

FX – x-ray fluorescence spectroscopy

GC – gas chromatography

GDP – gross domestic product

HC – hydrocarbons

HDAr – hydroaromatization

HDM – hydrodemetallation

HDN – hydrodenitrogenation

HDS – hydrodesulphurization

HDT – hydrotreatment

HPA – heteropolyanion

HYD – hydrogenation

IR – infrared spectroscopy

LHSV – liquid hourly space velocity

LOI – loss on ignition

MS – mass spectroscopy

PD – packing density

RT – room temperature

TG – thermogravimetric analysis

WUV – water uptake volume

XRD – x-ray diffraction

(This page was intentionally left in blank)

1. Introduction

The tightening of liquid fuels' specifications and the use of lower quality crude oils call for a constant effort to develop better performing hydrotreatment catalysts, which accounted for about 35% of the refining catalysts market in 2013.

In this context, this work aims to study the production of hydrotreatment catalysts by a simplified production method that combines support shaping and metal precursor introduction in the same step, named co-mixing. Furthermore, co-mixing is reported to provide a better dispersion of the metal species trough the support and allows the complications of impregnation to be avoided.

On a first stage, non-promoted catalysts were produced by co-mixing using a traditional mixing protocol and classical molybdenum precursors. A reference catalyst was also prepared by impregnation. The products were characterized and tested for catalytic performance.

In a second approach, the co-mixing procedure was combined with the use of a specific Mo precursor. To do so particular mixing conditions would have to be used. Therefore it had to be tested whether or not it was possible to do the shaping respecting that restriction, so a set of trial supports were produced and characterised texture wise.

After successfully applying the specific mixing conditions to support shaping, non-promoted and promoted catalysts were prepared by co-mixing with the specific Mo precursor. Again impregnated catalysts were produced to serve as reference. These catalysts were also characterized and tested for catalytic performance.

This report offers first a review of the hydrotreatment process, classical catalyst preparation and characteristics including a presentation of support preparation. This constitutes Section 2. In this section information regarding the application of the co-mixing technique and the use of a specific metal precursor is included as well as the objectives of the work and pursued strategy.

Section 3 begins with a listing of the products synthesised followed by a description of the experimental procedures employed and of the characterization techniques used.

The results and their discussion constitute Section 4. The products were divided in groups according to the strategy behind their production for a clearer presentation. For each group of products the results of the characterization are presented and discussed, then the results of catalytic testing (except for the support group) are interpreted considering that characterization. An intermediate conclusion for each group is given to resume the main results.

The final Section 5 presents the general conclusions of the work and perspectives of further development.

(This page was intentionally left in blank)

2. Literature review

2.1 Context of the work

2.1.1 Fossil Fuels Panorama

The energy demand and consumption can be naturally linked to population growth and increasing development of certain countries such as India and China. As Figure 1 shows, increasing world population and Gross Domestic Product (GDP), as a measure of development, can be expected to cause a 25% rise in global energy demand by 2040, despite the gains in energy efficiency. [1]

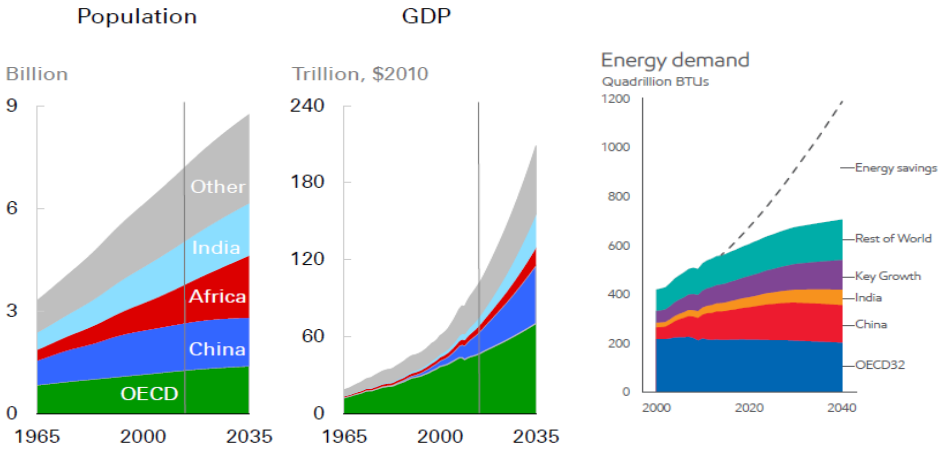

Figure 1 - Population and GDP growth (1965-2035) and Energy demand evolution (2000-2040) [1]

Fossil fuels are and should remain the main source of energy, with oil at the top despite a decrease in its share. The road transport sector is responsible for 44% of oil demand (2014) and its growth acounts for more than one third of the global demand evolution, followed by the industry and petrochemical sector with 26% (2014). This shows the importance of liquid fuels, namely light and middle distillates that are the most desired refinery products. Figure 2 indicates that gasoline and gasoil are the most wanted products, with heavy fuels showing a decrease in demand. [2]

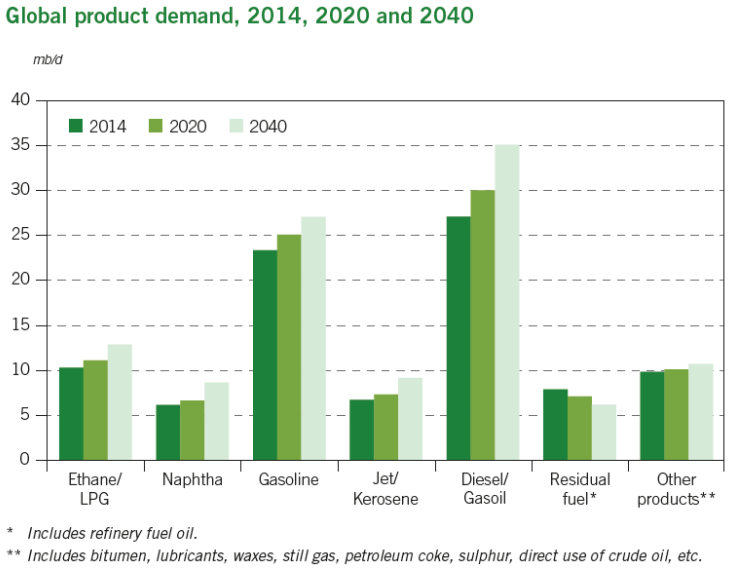

Figure 2 - Global demand by refinery product [2]

However, the crude oils available to refiners do not have a product distribution that corresponds to the market needs nor the quality to meet product specifications. Most crudes are expected to evolve becoming heavier and with a higher sulphur content. This forces refiners to use conversion and treatment processes to turn heavy fractions to valuable light and middle destilates and to remove heteroatoms, respectively. [3]

Regarding heteroatoms in crude oil, sulphur is the most abundant impurity with its contet ranging from 0,1 to 5 %(w/w) depending on the origin of the crude. The nitrogen content can be between 0,1 and 1%(w/w) and oxygen content is lower, usually up to 0,1%(w/w). Carboxylic acids are the main oxygen compounds and their presence causes corrosion problems for refiners. The most present metals are nickel and vanadium, them being mostly concentrated in the atmosferic and vacuum resids. [4]

2.1.2 The need for hydrotreatment

Although the technology was already known, it was only in the 1950's that commercial hydrotreatment (HDT) processes appeared due to the existence of a practical hydrogen source, it being the catalytic reforming units [5]. One of the first uses for hydrotreatment was running heavy naphtha to be fed to catalytic reforming, given that the platinum containing catalyst used in that unit is poisoned by sulphur, nitrogen and metal containing compounds. [6]

In alliance with the market and crude feed tendencies previously indicated, new legislation with the goal of reducing air pollution caused an increased need for hydrotreatment and a growth in the use of this process.

The Council Directive 70/220/EEC for the European Union was the beginning of a series of directives aiming to set the emission standards for motor vehicles, with the consecutive and more restringing stages of the legislation being referred to as Euro 1 (1992) to Euro 6 (2014) for light weight vehicles. The emission parameters presently limited by legislation refer to carbon monoxide, hydrocarbons, nitrogen oxides and particulate matter. [7] To obey these restrictions, the car manufacturing industry had to adapt with new technology, namely catalytic converters that are poisoned by lead and sulphur.

Later, Council Directive 93/12/EEC introduced mandatory fuel specification standards defining, among other, the maximum lead and oxygen content in gasoline and sulphur and aromatic content in both gasoline and diesel, as well as octane and cetane number respectively. This allowed for the generalized use of catalytic converters but caused major changes in the refineries considering that the limitations on lead and aromatics, particularly benzene, meant that the necessary octane number for gasolines had to be achieved by use of other components (ETBE, MTBE) that required new processes. The legislation became more rigorous with time and successive revisions, so that presently the maximum sulphur content in fuels is 10 ppm. [7]

Therefore, these factors have come together in making hydrotreatment one of the most important process units in a refinery, considering that at least 50% of refinery streams undergo HDT. [4]

2.1.3 Hydrotreatment process and its uses

The following reactions are common to all HDT units: hydrodesulphurization (HDS); hydrodenitrogenation (HDN); hydrodemetallation (HDM); hydrodearomatization (HDAr), included in hydrogenation (HYD), and hydrodeoxygenation. These reactions are all exothermic and, despite having different proposed mechanisms, consist of the hydrogenolysis of the heteroatomic compounds and the hydrogenation of the inorganic species (ex. sulphur to H_2S). In some mechanisms there is also hydrogenolysis of the unsaturated organic compounds that are created. [8]

The most usual reactor for hydrotreatment is a fixed bed down flow reactor with multiple beds and intermediate hydrogen quenching [4], although a traditional fixed bed reactor can be used for light feedstocks such as straight-run naphtha [6].Even though hydrogen is added to the feedstock prior to the reactor entrance, the H_2 quench is used to control the temperature in the reactor given that the reactions are exothermal. These units work in gas phase if feed is naphtha or kerosene and gas/liquid phase if diesel or heavier fractions.

To these reactors apply the classical disadvantages of fixed bed reactors, such as the need of shutting down the unit for catalyst replacement/regeneration, plugging of the bed and lastly the need of a catalyst that withstands the bed weight and provides an acceptable pressure drop as well as having a life time in terms of deactivation suitable for the operation of the process.

A general diagram of the process is depicted in Figure 3. The feedstock is mixed with hydrogen after being pre-heated by the product stream and then heated in a furnace prior to entering the reactor. The product stream goes through a gas-liquid separator to recover unreacted H_2 and the gaseous products, H_2S and NH_3. The latter must be separated from the hydrogen to be recycled. Lastly, a fractionation column separates the liquid products.

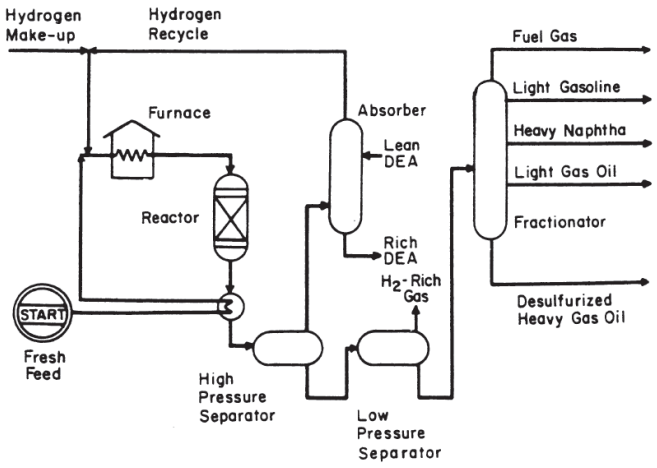

Figure 3 - Typical hydrotreatment process diagram [4]

Not so common, ebulated bed reactors can be used for very heavy feed such as vacuum resid. [4] These avoid the operation limitations that fixed bed reactor face when using heavy fractions, those being fast coke formation (and therefore deactivation) as well as plugging of the fixed bed. However, temperature control is more complicated, additional investment must be made on cyclones to separate

solid particles from the product stream and the catalyst must withstand the attrition and avoid agglomeration. [8]

Typical operation conditions depend on the feedstock, with heavier streams requiring a more severe treatment. As an example, a unit running a naphtha feed may operate at 320°C and 10 to 20 atm of H_2 partial pressure whereas a unit treating a vacuum gas oil (VGO) can be at 360°C, with 50 to 90 atm of H_2 partial pressure and a space time velocity that can be 4 times lower than in the previous case. [4]

As mentioned before, HDT is one of the most relevant processes in a refinery, with Figure 4 illustrating its various applications. Although the reactions that occur are always the same, different units serve diverse purposes to which they are adjusted to.

Table 1 summarizes the most common objectives of HDT for the different types of refinery streams.

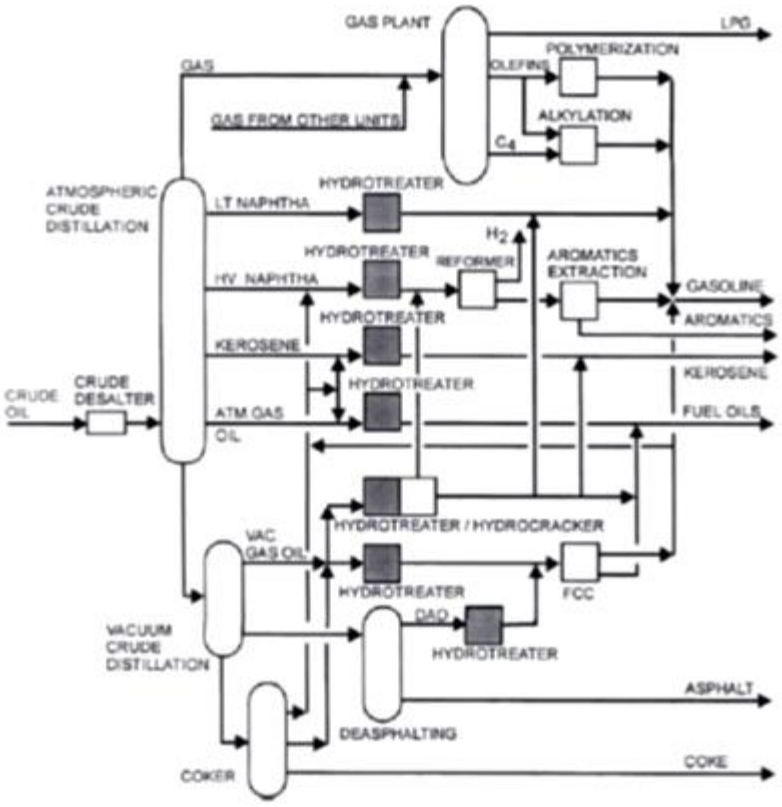

Figure 4 – Schematic diagram of a deep conversion refinery highlighting the abundancy of HDT units [4]

Table 1 - Main goals for hydrotreating of different refinery streams [4] [5] [6]

Stream	Objective of HDT	Reaction
Straight-run streams	Improve odor	HDS
Light naphtha	Reduce sulfur content	HDS
Catalytic reformer naphtha feed	Avoid catalyst poisoning	HDS, HDN, HDM
Hydrocracking feed		
Diesel	Meet product specifications (sulfur content and cetane number), improve stability	HDS, HYD
Kerosene	Meet product specifications (ex. smoke point), improve stability, reduce corrosiveness	HDS, HDN,HYD
Resids	Reduce viscosity, metal load and sulfur content	HDS, HDM

In newer applications, HDT can also be used in the production of biofuels. An example is the *Vegan* process by Axens, in which vegetable oils undergo hydrotreatment to remove the oxygen atoms and thus obtain paraffins. These can be further refined into liquid biofuels. [9] This technology will be employed at the La Mède refinery operated by Total. [10]

2.1.4 Hydrotreatment catalysts

The tightening of liquid fuels' specifications and the use of lower quality crude oils call for a constant effort to develop better performing and long lasting HDT catalysts. In fact, these catalysts accounted for about 35% of the refining catalysts market in 2013. [11] Therefore, this is a very active field of research, with many advances being done thanks to characterization techniques and modelling, namely in understanding the nature of the active phase.

Hydrotreatment uses mono-functional supported catalysts, typically of Mo or W with Ni or Co as promoters over gamma alumina. [12] The CoMo, NiMo and NiW families are the most common. [4] An alternative support will be silica-alumina. The catalyst is active when the metals are in sulphide form, thus being called catalysis by Transition Metal Sulphides.

The choice of catalyst naturally depends on the main objective of the unit: CoMo is indicated for HDS at low pressure, NiMo for HDN as well as HDM and HDS at high pressure and finally NiW for HYD. [5] [6] The preferential use of alumina as support is related to this material allowing good dispersion of the active phase and to its mechanical properties. [13] Concerning the support texture, for heavier feeds a larger pore diameter is needed for the diffusion of big molecules as well as an increased pore volume to allow for metal deposition. [12] Different catalyst shapes and sizes are available, from cylinders and rings to trilobes, the choice depending on reactor operational factors such as pressure drop and

plugging. It is not uncommon to have distinct beds along the same reactor, with different active phases and/or sizes, such as larger particles in the top and bottom of the reactor (zones prone to plugging and pressure drop limited). [12]

General catalyst characteristics are: 1-6%(w/w of catalyst) of promoters Co or Ni; 8-30% of Mo; 17-35% of W; surface area of 100-400 m^2/g; pore volume of 0,6 to 1,0 mL/g; narrow pore size distribution with mesoporosity for non-residue feeds. [4] [5] Usually an optimum pore diameter can be found, given that smaller diameters give haze to diffusional limitations and with larger ones surface area decreases. [14]

Several mechanisms can be attributed to loss of activity: sintering and decomposition of the active phase, poisoning (by Na, Ca, As), coking and deposition of metals, being the last two the main causes for deactivation. [5] [8] [13]

2.1.4.1 Catalyst Synthesis

As for catalyst synthesis, the conventional procedure includes impregnation of the support with metal precursor solutions followed by a maturation step and thermal treating (drying and eventually calcination), finally sulphidation of the metallic phase is necessary to achieve an active catalyst. [15] A more detailed description of some of these steps follows.

2.1.4.1.1 Impregnation

Impregnation is a key step in preparing supported catalysts, with different techniques being available. [15] One of the most commonly used for the preparation of HDT catalysts is dry impregnation; also called incipient wetness impregnation.

In dry impregnation the solution of metal precursors is prepared so as to have se same volume as the pore volume of the support, ensuring the deposition of all species solubilized and avoiding any filtration steps. The promoter can be impregnated at the same time as the metal, called co-impregnation, or by successive impregnations. [15] Classical metal precursors are polyoxometalates (iso or heteropolyanions) of Mo or W and Ni or Co salts.

After impregnation a maturation step allows for complete diffusion of metal species trough the pores achieving a homogeneous distribution of compounds along the extrudate.

Impregnation is a complex operation with various phenomena playing in the deposition of the metal precursors (chemisorption, electrostatic interactions). In the particular case of Mo over an alumina support, the pH and concentration dependent equilibrium of Mo species in aqueous solutions (Figure 5) and the Point of Zero Charge of alumina (approximately at pH 9) will greatly influence the final outcome of the impregnation.

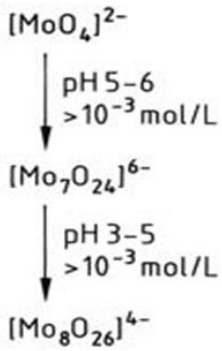

Figure 5 - Partial scheme of molybdenum aqueous chemistry [16]

The case of impregnation of ammonium heptamolybdate $(NH_4)_6Mo_7O_{24}$ is a good example. This molybdenum compound was one of the first precursors widely used in industrial production. During impregnation of ammonium heptamolybdate, stable at low pH, acid-base reactions with surface hydroxyl groups associated with the buffer effect of the support at pH 9 cause conditions propitious to the formation of monomolybdate MoO_4^{2-} in the pores. Bellow the Point of Zero Charge, using a sufficiently acidic solution, a partial dissolution of the support may occur leading to the formation of the heteropolyanion (HPA) or polyoxoxmetalate $Al(OH)_6Mo_6O_{18}^{3-}$ that will be at the surface of the support after drying and may precipitate in the pores. [15]

Using conventional impregnation and precursors it is difficult to control the nature of the deposited species and to guarantee good dispersion of the metal throughout the support. [12]

As the impregnation will be dependent on HPA chemistry in the pores of the support, the direct impregnation of with HPA species solutions has been used to prepare efficient catalysts. HPAs that have both Mo and Co/Ni can be used, with the advantage of having the two metals deposited in the same cluster. [15]

The thermal treatment of calcination is used, after drying, to eliminate precursor counter ions and to form a dispersed metal oxide phase. Yet, this procedure is not a necessary step, as catalysts may be activated after drying, and calcination may even damage catalytic activity by promoting sintering of the metals or the formation of stable oxides that are difficult to sulphide. Currently, since organic additives are used during or after impregnation to interact with the metals (complexing agents are an example), calcination is not employed. [15]

2.1.4.1.2 Sulphidation

As mentioned above, sulphidation is the step where the active metal sulphided phase is created. Industrially, the catalyst may be sulphided *in situ,* usually in the presence of feedstock spiked with a sulphiding agent (dimethyl disulfide is a common example), or it can be sulphided *ex situ* avoiding the handling of sulphur compounds in the refineries. At laboratory scale gas phase sulphidation with an H_2/H_2S mixture is most often performed. [15]

Two main mechanisms have been proposed for sulphidation resulting in MoS_2, one considering a MoS_3 species as intermediate and another where the intermediate is an oxysulphide MoS_xO_y. [15]

In any case, the nature of the starting metal species and the sulphidation procedure itself have a great impact on the formation of the active phase and its distribution on the support surface, which in turn will rule the catalysts performance. [15]

2.1.4.2 Active phase

Regarding the active phase, for non-promoted catalysts, it can be said that it consists of MoS_2 mono-layers (slabs) dispersed over the alumina surface. The shape of the MoS_2 slabs will depend on the relative energy of the two different types of edges, and is hexagonal in HDS conditions, as shown in Figure 6. [15]

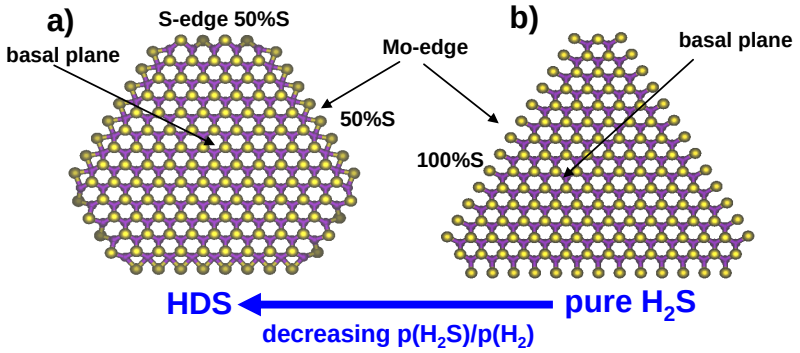

Figure 6 - Morphologies of non-promoted MoS_2. [15]

For promoted catalysts, the generally accepted model to describe the active phase is the Co-Mo-S model (also applicable to the NiMo system). The Co-Mo-S phase is a structure similar to the MoS_2 layers with the Co atoms at the edges in substitution of Mo atoms. The Co-Mo-S layers are also hexagonal in HDS conditions and Ni-Mo-S layers will be deformed hexagons. [15] Different promoter atoms in the same Co(Ni)-Mo-S slab may not have the same properties due to various effects such as diverse geometries or sulphur coordinations at the edge. [4] The decorating of the edges by the promoter will also vary: Co is more stable on the S-edge and Ni is more stable in the Mo-edge. [15]

Distinction may be made between two types of Co-Mo-S phase. Type I Co-Mo-S refers to mono-layers with a strong interaction with the alumina support, with maybe even Al-O-Mo type bonds. On the other hand, Type II Co-Mo-S will be a multiple-slab phase with weak interactions with the support that shows enhanced activity. [4] [13] However it should be noted that the relationship attributed between Type II Co-Mo-S and slab stacking may be circumstantial, the stacking being dependent on the type (gas or liquid phase) and extent of sulphidation. [17]

Finally, the surface of an alumina based hydrotreating catalyst can be represented as in Figure 7 (figure 1.13 CTMS), in which the Co-Mo-S slabs are visible in hexagonal geometry with Co atoms at the edges. Other unwanted and not active phases are formed during the synthesis and activation of the catalyst, these being molybdate species for instance MoO_3 and $CoMo_2S_4$, cobalt sulphides such as Co_8S_9, non-promoted MoS_2 or cobalt in interaction with the support. [4] [15]

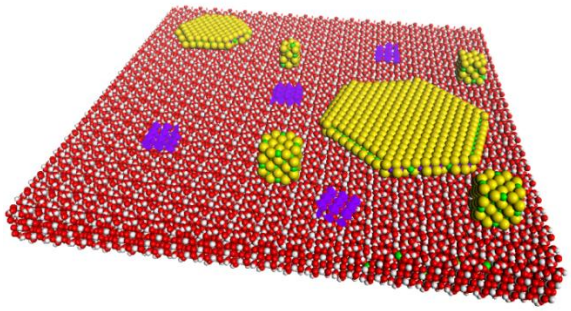

Figure 7 - Representation of the different species at the surface of a $CoMo/Al_2O_3$ catalyst. [15] Yellow-sulphur; Purple-molybdenum; Green-cobalt

The promotion effect, meaning increased activity, provided by the addition of Co or Ni may be explained if one considers that the activity is related to the "metal-sulphur" bond energy. [18] The promoter metals lower the "metal-sulphur" bond energy which causes an increase in activity in comparison with non-promoted catalyst, as Figure 8 shows.

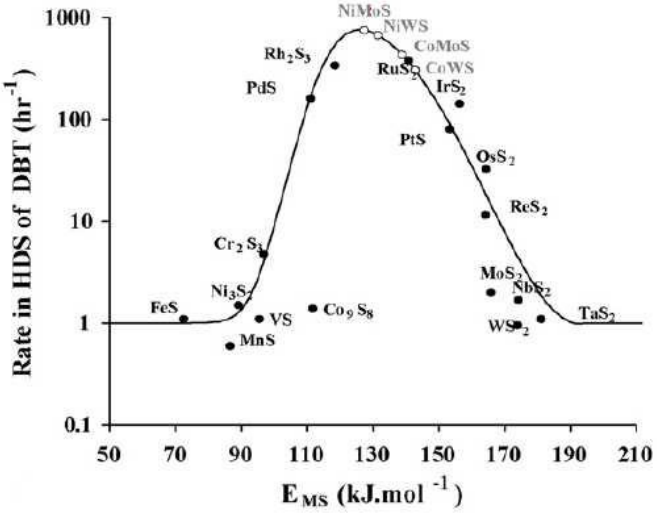

Figure 8 - Activity of various metal sulphides for dibenzothiophene HDS as a function of "metal-sulphur" bond energy [19]

This explanation for the promotion effect is rational if one considers what the active sites are in fact. It can be said that the active sites are coordinative unsaturated sites (CUS), namely sulphur vacancies, along the edges of the slabs. These CUS sites will be of different nature depending on their geometry and placement on the edge and various sites will not have identical roles in all the HDT reactions.

As an example, a HDS reaction may have a mechanism in which the adsorption of the reactant is made through the sulphur atom at a sulphur vacancy. Considering still HDS, hydrogen will be needed at some point, so it is considered that H_2 may be adsorbed dissociatively over the active phase forming SH groups. The adsorption of hydrogen can also promote the formation of the sulphur vacancies, as shown in Figure 9.

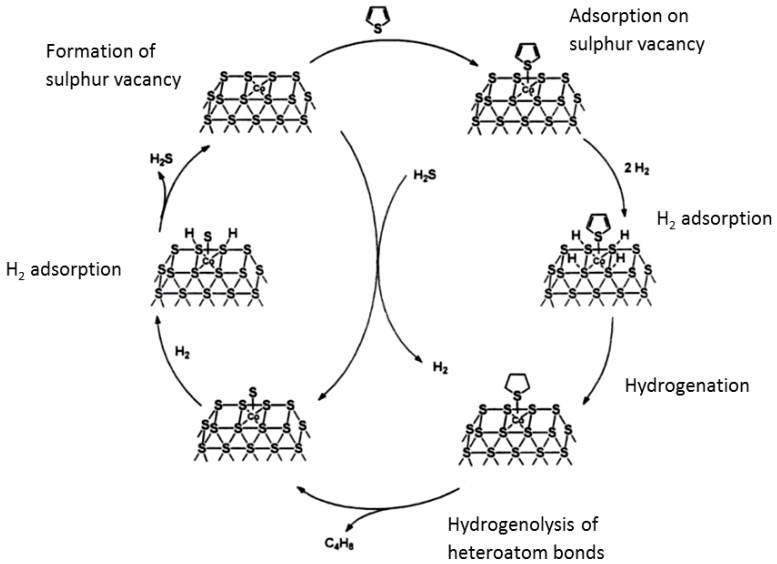

Figure 9 - Proposed mechanism of thiophene HDS highlighting the role of H_2 adsorption and sulphur vacancies. Adapted from [4]

Another type of active sites would be the "brim" sites. These are sulphide clusters in the basal plane of the slabs, the row of S atoms right next to the edge, with high electronic density that provides them with a metallic-like character. These were observed for both non-promoted and promoted catalysts by Scanning Tunneling Microscopy (STM), as Figure 10 shows, and the same image was obtained by simulation. These sites should be able to adsorb and hydrogenate some reactants, but are not able to cut the bond C-heteroatom. Nevertheless, it should be considered that the conditions used for STM, including the samples, are very different from the ones in reaction media. [13] [15]

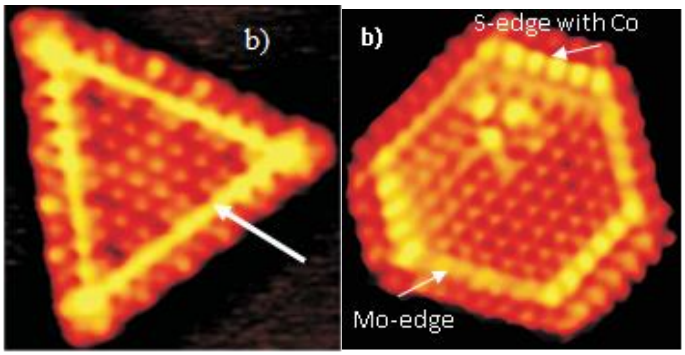

Figure 10 - MoS_2/Au (left), Co-Mo-S/Au (right); white arrows indicate "brim" sites [15]

2.2 Support synthesis and co-mixing

The catalyst support essentially defines its macroscopic shape and overall textural properties such as porosity and surface area. Also, the support's surface plays a major role in the dispersion of the active phase.

The synthesis of an alumina support starts with an alumina precursor powder that suffers a shaping step followed by thermal treatment, calcination, when the alumina is formed.

2.2.1 Boehmite

For hydrotreatment catalysts, a usual alumina precursor is ɣ-AlOOH, boehmite, which is an aluminium oxyhydroxide. [15] Its crystal structure is represented in Figure 11, each Al atom being surrounded by a distorted octahedron of O atoms, building layers connected by hydrogen bonds. [14] A poorly crystallized form of boehmite, called *pseudoboehmite*, is also used as ɣ-Al_2O_3 precursor. [20]

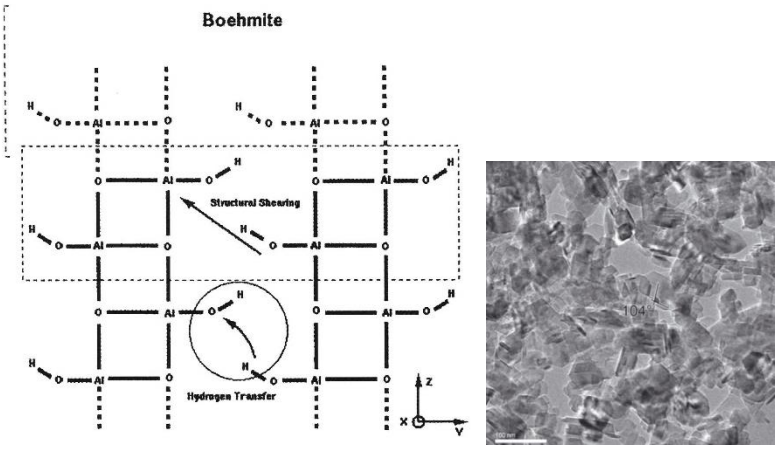

Figure 11 - Structure of boehmite and processes leading to transformation into alumina (left) [14]; TEM image of boehmite crystallites (right) [21]

Two production methods are used for obtaining boehmite for catalyst synthesis [15]:

a) From aluminium alkoxide:

$$Al(OR)_3 + 2H_2O \rightarrow 3ROH + AlOOH\downarrow \text{ Equation 1}$$

This method produces high purity boehmite, without common contaminants like sodium or silica. Industrially, the boehmite tradenames Pural and Disperal by Sasol, among others, are synthetized using this pathway.

b) Precipitation of aluminium salts in aqueous solution:

$$Al_2(SO_4)_3 + 3NaOH \rightarrow 2AlOOH + H_2O + 3Na_2SO_4 \text{ Equation 2}$$

Using this method gives way to boehmite powders with a relatively higher impurity content due to the counter ions, which must be monitored for synthesis of catalysts poisoned by the elements in question (as HDT catalysts are poisoned by sodium).

In either case, many parameters of the production process can be manipulated to change the properties of the produced boehmite.

The boehmite powder is subjected to a shaping stage in which a paste of adequate rheological properties is formed by adding water in combination with inorganic and/or organic compounds. The paste is then extruded into the desired shape and size.

2.2.2 Shaping

2.2.2.1 Mixing and shaping

The previously mentioned paste is made by a process named mixing, kneading or mulling, which aims to disperse the powder, dealing with the different possible textural entities of boehmite. Those are [14]:

a) Primary Particles/Crystallites: smallest entity; $2<d_p<50$ nm

b) Aggregates/Primary aggregates: assembly of primary particles chemically connected by Al-O-Al bridges; $30< d_p <500$ nm

c) Agglomerates: assembly of aggregates held together by physical and electrostatic forces (van der Waals, hydrogen bonds); $5\mu m< d_p <10\mu m$

d) Powder: assembly of agglomerates; $d_p=40\mu m$

The powder particles and agglomerates can be “broken down” into aggregates by mechanical force provided by the mixer. To cause deaggregation mechanical force is not enough to break the chemical bonds that hold the aggregates together, for this a chemical attack is needed. Mixing with an acid solution will bring forth deaggregation and peptization of the resulting primary particles.

Peptization, in a general way, consists on creating a positive net charge on the surface of the boehmite crystallites preventing them from coalescing or settling by electrostatic repulsion. With the Point of Zero Charge of boehmite being at approximately pH 9 [22], just as alumina, peptization is achieved when the mixture is bellow that point by the use of an acidic solution. [14] It is also suggested that some degree of dissolution may be necessary for efficient peptization. [22]

The process of peptization is still not a clear one, nor is the relationship between the mixing conditions and the final texture of the support produced. However, it is accepted that peptization reduces larger pores due to deaggregation and that the smaller particles thus obtained rearrange in some sort of long range order. So, a higher peptization degree may be expected to eliminate macroporosity and provide a slender pore size distribution on the mesoporous area. [22] [23]

The mixing with the acidic solution, acid mixing, may be followed by an optional step of neutralization. For neutralization a basic solution is added to the paste being mixed, but the amount of base is inferior to the amount of acid previously used. During this step a new change in surface charges can cause some new agglomeration. [24]

The overall phenomena of peptization and neutralization is represented in the scheme of Figure 12.

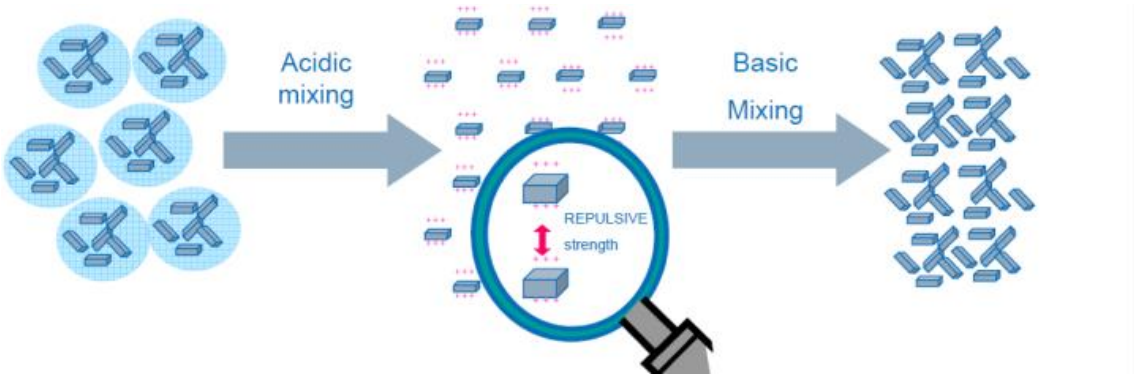

Figure 12 - Scheme of peptization

The final textural properties of the support depend not only on the mixing step but also on the properties of the boehmite powder used, naturally. Here not only the crystallite's shape and size but also the concept of dispersibility is considered.

The dispersibility of a powder depends on the cohesion of the aggregates. For the same amount of peptizing agent, such as an acid, the powder is less dispersible if the bonding between the aggregates is stronger. [14]

Karouia *et al* [24] studied the textural properties (pore size distribution in the mesoporous range by nitrogen physisorption) of three boehmites with different dispersabilities at the various stages of the shaping process, namely of the synthesized boehmites, of the product after acid mixing, of the product after neutralization and of the dried extrudate.

They found for a boehmite with low peptization ability, a wide pore size distribution, similar at any point in the process, attributed to a heterogeneous arrangement of aggregates. For a boehmite with medium peptization ability the pore size distribution varies throughout the shaping process and it is narrower. Finally the highly dispersible boehmite showed the narrowest pore size distribution and lowest mean pore diameter, with slight differences at each step, this behavior being attributed to a change of arrangement of crystallites during peptization but a regression to the initial arrangement after neutralization.

In conclusion, the mixing step plays a complex and important role in the texture of the final support by the choice of conditions such as mixing potency and acid choice and quantity. However, the properties of the initial powder also condition the mixing parameters and the final texture obtained.

2.2.2.2 Extrusion, drying and calcination

The paste obtained by mixing is then extruded through a die plate with the desired shape (cylindrical, trilobe, etc.). The extrusion process does not impact on the texture of the support. [24] At this point the extrudate obtained is pliable just like the paste and must be dried. During the drying there is only the loss of free water and the solid dried extrudates are not the finished product since they are still made of boehmite.

It is during calcination that the topotatic transformation, meaning without change of crystallite morphology, from boehmite to ɣ-Al_2O_3 takes pace by removal of structural water. [15]

The ɣ polymorph is formed at a temperature of 500°C and up to 700°C. A higher calcination temperature is linked to a decrease of surface area and an increase in pore diameter. [14]

2.2.3 Alumina

Alumina is the aluminium oxide Al_2O_3. There are many transition aluminas that trough thermal treatment will all transform into the stable phase of aluminium oxide that is α-Al_2O_3. [14] Figure 13 exemplifies these transitions starting from the various aluminium hydroxides that serve as alumina precursors.

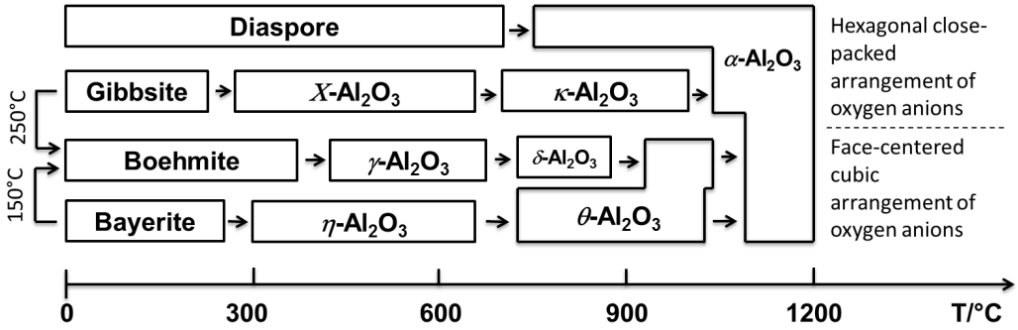

Figure 13 - Scheme of the different alumina polymorphs, their relationship and temperature stability range [25]

The transition aluminas are the ones most often used as catalyst supports, with ɣ-Al_2O_3 being used in HDT catalysts due to its thermal stability in the range of operational temperatures, mechanical properties and ability to withstand traditional impregnation.

It has been suggested that ɣ-Al_2O_3 has a spinel type structure with oxygen in a close-packed lattice, however there is still discussion on the location of the vacant cation positions implied by stoichiometry. [14] Figure 14 schematizes this structure.

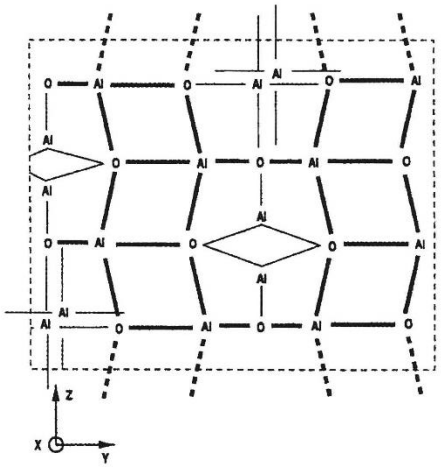

Figure 14 - Schematic of alumina structure [14]

2.2.4 Co-mixing

Co-mixing refers to the addition of the metal precursor during the production of the support. This can be used to avoid the previously mentioned disadvantages of impregnation, to reduce the total number of manufacturing steps, especially high energy consuming operations like drying, or to allow for higher metal loadings in combination with impregnation.

This process is referred to as a possible path to the production of HDT catalysts [5] [6], and it is said to ensure a good distribution of the active metals in the support. [12] It is also necessary to ensure that the textural and mechanical properties of the final product are adequate.

There are some examples of the use of this technique in the literature. Kemp and Adams [26] succeeded in preparing catalysts with a metal efficiency greater than that of conventionally prepared catalyst by mixing the metal precursor (nickel nitrate and ammonium molybdate) solution with a boehmite hydrogel for 2h forming a slurry followed by filtration and extrusion. However, in the filtration step molybdenum is lost in the liquid, especially when the pH of the slurry is higher than 8, this being attributed to repulsion between the negatively charged boehmite crystallite surface and the Mo anions.

Process patent US4097413 [27] describes the synthesis of desulphurization catalysts by co-mixing a solution of ammonium heptamolybdate with boehmite to form a damp powder that is then dried and co-mixed again with a solution of a suitable cobalt salt to produce an extrudable paste. It is claimed that this method can produce catalysts with metal loadings up to 30%MoO_3, but there is no gain in process simplicity.

Another process patent, US4402865 [28], also describes a path to obtain high metal loading catalysts by peptizing boehmite with a polyprotic acid such as sulphuric acid, then co-mixing of a Co or Ni compound followed by neutralization and co-mixing with a Mo species. Yet, none of the examples indicate the catalyst performance.

Other relevant work is that of Amaroli and Minoux [29], in which the interaction between Mo and boehmite was studied using a Pural SB boehmite sol with added heptamolybdate. They found that the interaction between Mo species and boehmite is stronger than a pure electrostatic one, suggesting an iono-covalent type interaction, and that the most basic hydroxyl groups preferentially interact with the metal. Also, the topotatic transformation of boehmite to γ-Al_2O_3 does not seem to be affected by the presence of Mo.

2.3 Objectives and work strategy

The objective of this work is to produce hydrotreatment catalysts by co-mixing that at least perform like conventional ones and that have adequate textural properties, offering a simplified production method as alternative to the currently used and/or a method for production of high metal load catalysts in combination with impregnation.

On a first approach, conventional molybdenum precursors, namely ammonium heptamolybdate and molybdate trioxide with phosphoric acid, were used for co-mixing in normal mixing conditions with two

different boehmite powders to produce non-promoted catalysts. The products were characterized and tested for toluene hydrogenation to evaluate the impact of the synthesis on their performance.

The second strategy was to use a specific Mo precursor and particular mixing conditions. Those mixing conditions were first tested by producing a series of supports. Later they were applied to the co-mixing of the specific Mo precursor to produce non-promoted and promoted catalysts. These catalysts were also characterized and subjected to catalytic testing by toluene hydrogenation.

3. Experimental Part

The catalysts synthesised were divided into four groups according to their nature and objective behind their synthesis. The groups are: Catalyst Set 1; Trial Supports; Catalyst Set 2 and Catalyst Set 3.

In Catalyst Set 1 are grouped the products synthesised to test the first strategy of co-mixing in conventional conditions (acid mixing and neutralization) with conventional metal precursors, ammonium heptamolybdate and molybdenum oxide plus phosphoric acid. The co-mixing was done using two different alumina precursors (boehmite): Pural SB3 from Sasol and Powder X (includes nitric acid in its composition). Other than the co-mixing products, a catalyst prepared by impregnation of heptamolybdate was synthesised to serve as reference.

The Trial Supports are the supports prepared to test particular mixing conditions. Catalyst Set 2 and Set 3 group the non-promoted and promotes catalysts, respectively, prepared by co-mixing of a specific Mo precursor with the particular mixing conditions.

An overview of these products is presented with some schemes to clarify the preparation method. The different techniques and processes applied in catalyst synthesis are described, followed by some information regarding all the characterization techniques employed.

3.1 Overview of prepared products and analysis performed

The products are listed here using the nomenclature employed throughout this work:

a) For supports: *alumina precursor condition*, for example Powder X Conv. The mixing conditions are noted by *Conv* (conventional).

b) For co-mixing catalysts: *metal precursor+alumina precursor condition*, for example MoP+Pural SB3 Conv.

c) For impregnated catalysts: *metal precursor/alumina precursor condition*, for example Mo_7/Powder X Conv.

The nomenclature is referred again when the corresponding techniques or conditions are described in the following sections.

In some cases a scheme is presented. The reference used corresponds to the catalyst, which was catalytically tested, represented in the orange box. Other samples, such as a calcined or sulphided catalyst, were prepared for characterization only and were not used in the catalytic test. The preparation steps are indicated by arrows in blue. The characterizations performed on each sample are indicated in black.

3.1.1 Catalyst Set 1 group

These are the catalysts synthesised by co-mixing in conventional way (acid mixing and neutralization) with conventional metal precursors, ammonium heptamolybdate and molybdenum oxide plus phosphoric acid, according to the first strategy employed, and a catalyst prepared by impregnation as reference.

The catalysts are the following:

Mo7+Pural SB3 Conv: Catalyst prepared by co-mixing of heptamolybdate and Pural SB3 in conventional conditions.

MoP+Pural SB3 Conv: Catalyst prepared by co-mixing of molybdenum trioxide and phosphoric acid with Pural SB3 in conventional conditions.

Mo7+Powder X Conv: Catalyst prepared by co-mixing of heptamolybdate and Powder X in conventional conditions.

MoP+Powder X Conv: Catalyst prepared by co-mixing of molybdenum trioxide and phosphoric acid with Powder X in conventional conditions. A scheme of the different operations performed and obtained products is presented in Figure 15. An equivalent scheme is applicable to the previously listed catalysts, with the respective difference in the mixing components. Also, the XPS analysis of the sulphided catalyst was only performed for MoP+Powder X Conv.

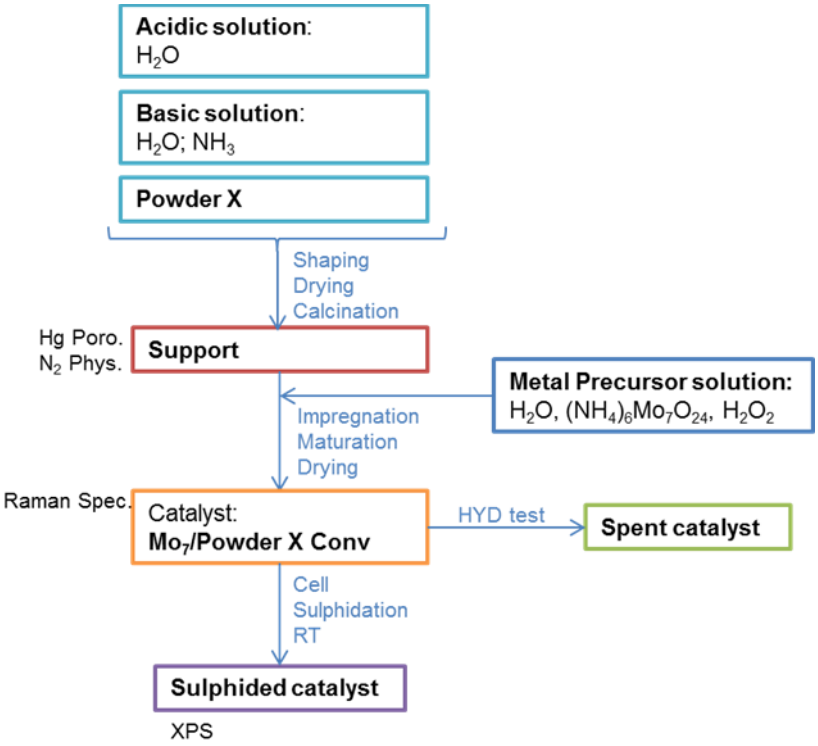

Figure 15 - Scheme of catalyst preparation by co-mixing of molybdenum trioxide and phosphoric acid with Powder X in conventional conditions, MoP+Powder X Conv

Mo7/Powder X Conv: Catalyst prepared by impregnation of a conventional Powder X support with heptamolybdate. The impregnated catalysts are identified by a notation of "metal precursor"**/**"support". Figure 16 presents a scheme of the production of this catalyst.

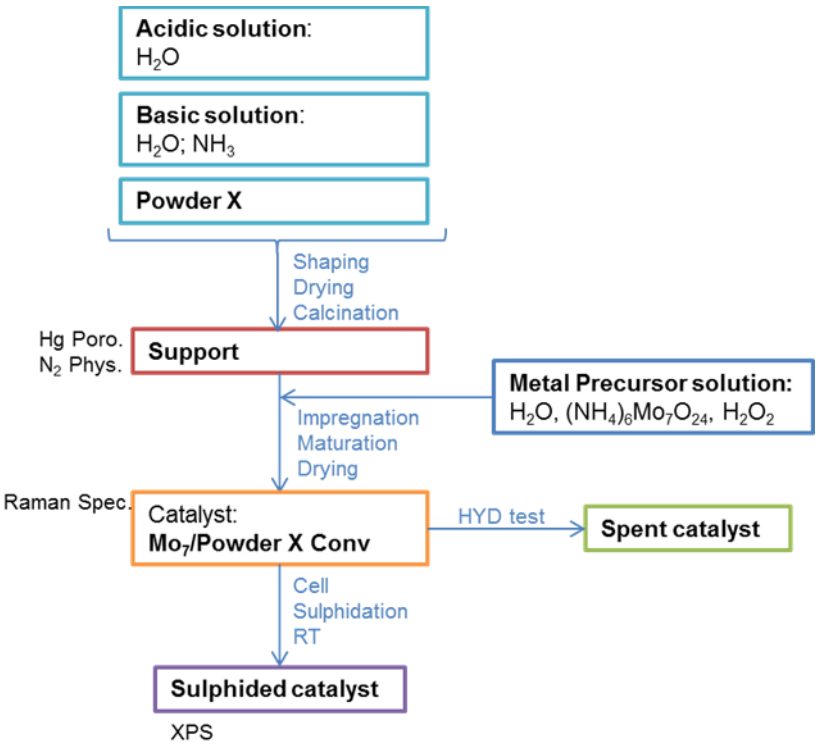

Figure 16 - Scheme of catalyst preparation by impregnation of a conventional Powder X support with heptamolybdate, Mo_7/Powder X Conv

3.1.2 Trial Supports group

Seven supports were prepared to test the mixing using particular conditions and textural analysis, Hg Poro. and N_2 Phys., were performed on the calcined extrudates.

3.1.3 Catalyst Set 2 group

Nine non-promoted catalyst were produced by co-mixing of a specific Mo precursor in particular mixing conditions. Two catalysts were prepared by impregnation to serve as references.

3.1.4 Catalyst Set 3 group

Two promoted catalysts were synthesised by co-mixing with a specific Mo precursor in particular mixing conditions. A catalyst prepared by impregnation was used as reference.

3.2 Procedures used for support and catalyst preparation

3.2.1 Mixing and co-mixing

All mixing took place in a Brabender Mixer and all extrusions were performed in a MTS Systems vertical piston extruder at a speed of 1 cm/min using a cylindrical die plate of 2 mm in diameter. The extrudates are dried in a Binder oven at 80°C for at least 12h, typically overnight. When executed, calcination was at 540°C for 4h in a Naberthern muffle furnace, unless otherwise indicated. The properties of the used alumina precursors can be consulted in Annex 1.

3.2.1.1 Conventional Mixing

After filling the mixing bowl with the adequate amount of alumina precursor powder, a nitric acid solution is added in two minutes while the bowl contents are mixed at a speed of 16 rpm. The resulting paste is mixed for 30 minutes at 33 rpm, this being called the *acid mixing* stage.

When the acid mixing ends, a solution of ammonia is added at once. The paste is mixed for 15 minutes more at 33 rpm, this being called the *neutralization* stage. After recovering the paste from the mixing bowl it is extruded. The extrudates are dried and then calcined.

The acid and basic solutions are prepared so that the total amount of water used is equal to the amount of water needed to form a paste, and to have the desired amount of acid and base.

The quantity of water necessary to form a paste depends on the powder being used and is divided between the acid and basic solutions in a proportion of about 80%-20% respectively. This quantity of water is determined empirically by observation of the rheological properties of the paste during the mixing. Note that after acid mixing, with 80% of the water added, a paste is already formed.

Two different boehmite powders were used in these conditions: Pural SB3 and Powder X. Pural SB3 is a high purity boehmite synthetized from aluminium alkoxides commercialized by Sasol. Powder X is a boehmite used by catalyst making industries, which includes nitric acid in its composition.

The quantity of acid and base to be added in solution that is considered as *conventional* for each powder is indicated in Table 2.

Table 2 - Conventional quantities of acid and base for each boehmite

	Pural SB3	Powder X
HNO_3 (mmol/g Al_2O_3)	0,63	-
NH_3 (mmol/g Al_2O_3)	0,25	0,38

It should be noticed that for Powder X no acid is added in solution because, as mentioned, it already contains nitric acid in its composition in a quantity equivalent to 0,48 mmol HNO_3/g Al_2O_3. Also, these quantities are expressed on the γ-Al_2O_3 basis. The mass of alumina obtained from one gram of boehmite is known for each powder by determining the Loss on ignition (LOI). LOI is given by the powder mass difference before and after thermal treatment (1000°C for 3h) divided by the mass before the treatment.

All products with the label “Conv” (short for *conventional*) have been prepared by this procedure and/or with these quantities of nitric acid and ammonia.

3.2.1.2 Co-mixing

The procedure is in all the same as the one descried above with one exception. The acid mixing is performed with a metal precursor solution prepared as described in section 3.2.3 to which the necessary quantity of nitric acid was added. The concentration of the solution in metal and acid is adjusted so that the addition of the solution to the boehmite powder leads to the formation of a paste.

Catalysts prepared by co-mixing are identified with the label “metal precursor”+”alumina precursor”. For example, Mo_7+Pural SB3 means ammonium heptamolybdate co-mixed with Pural SB3.

In this case an organic binder Methocel is added to the powder to help produce an extrudable paste. The mass of Methocel used corresponds to 2% of the mass of Al_2O_3 used in the mixing.

3.2.2 Impregnation

Incipient wetness impregnation is performed using a metal precursor solution with the same volume as the porosity of the support. This is assumed to be equal to the Water uptake volume (WUV), which is obtained by adding distilled water to a known mass of support until it is evenly wet and starting to adhere to the recipient.

The WUV (mL/g) will be the quotient between the volume of water used and the initial mass of support. This way, for any given amount of the same support to be impregnated, the volume of solution to be prepared is given by the product between the mass of the support and the WUV.

The impregnation is performed by adding the metal precursor solution drop by drop onto the support, which is placed in a rotating recipient and mixed with a spatula to ensure even distribution of the solution. At the end of the impregnation all extrudates should be wet and show a homogeneous colour.

The maturation step follows, leaving the catalyst overnight in a Binder oven at 23°C and 95% humidity. Afterwards it is dried at 120°C for 24h in a Pol-Eko-Aparatura ventilated oven.

For impregnation, the support used was always calcined (540°C 4h) after drying of the extrudates.

The catalysts prepared by impregnation are noted by “metal precursor”/”support”, for example, Mo_7/Powder X Conv indicates the impregnation of a support of Powder X mixed conventionally with ammonium heptamolybdate.

3.2.3 Metal precursor solution preparation

Depending on the case, solutions with metal precursors were prepared either for co-mixing or for impregnation, with the quantity of water required for each technique.

The quantity of metal precursor was calculated in order to have catalysts with 10%MoO_3(w/w_{cata}). This is the conventional notation, even if no actual molybdenum trioxide is formed. The weight of the catalyst is defined as the sum of the oxide species that would be present after calcination. For example, for a non-promoted Mo catalyst this will be the mass of MoO_3 added to the mass of Al_2O_3 and for a promoted NiMo catalyst this will be the mass of MoO_3 added to the mass of NiO and of Al_2O_3, as Equation 3 shows.

$$\%MoO_3\ (w/w_{cata}) = \frac{mass\ MoO_3}{mass\ Al_2O_3 + mass\ MoO_3 + mass\ NiO} \quad \text{Equation 3}$$

It was assumed that all metal atoms would originate the respective oxide, meaning that one mole of heptamolybdate corresponds to seven moles of molybdenum trioxide, for example.

Again, to know the actual mass of Al_2O_3 in the weighted powder (in the case of co-mixing) or support (for impregnation) the Loss on ignition for each material is measured.

3.2.3.1 Ammonium heptamolybdate

The solutions were prepared using $(NH_4)_6Mo_7O_{24}\cdot 4H_2O$ from Merck and molar mass of 1238,86 g/mol and H_2O_2 30%(w/w) solution from Sigma-Aldrich. The hydrogen peroxide is used for a better dissolution of the molybdate.

The calculated amount of molybdate is dissolved in a fraction of the needed quantity of water and the hydrogen peroxide solution is added so that H_2O_2/MoO_3=0,5 (molar ratio). The final mass or volume of the solution is adjusted by adding water and it is homogenized again.

3.2.3.2 Molybdenum trioxide and phosphoric acid

The solutions were prepared using MoO_3 from Axens with a molar mass of 143,95g/mol and a phosphoric acid solution at 85%(w/w) from VWR Chemicals.

The calculated amount of molybdenum oxide, a fraction of the needed amount of water and the phosphoric acid solution are added to a round bottom flask. The quantity of phosphoric acid is calculated by the molar ratio P/Mo=0,45. The solution is left under reflux at 120°C and agitation in a Radleys Tornado IS6 until it is limpid. After cooling to room temperature the final mass or volume of the solution is adjusted by adding water and it is homogenized again.

With this P/Mo ratio, a Strandberg-type HPA, $P_2Mo_5O_{23}^{6-}$, could be expected to form in solution.

3.2.4 Gas phase cell sulphidation

The samples were sulphided at atmospheric pressure to be sent for analysis. The sulphidation was performed at two different temperatures with an H_2/H_2S mixture containing 15%(v/v) of H_2S from Air Liquide at a flowrate of 2 $L/h/g_{cat}$.

The cell sulphidation takes place in a laboratory hood with constant ventilation and equipped with a H_2S sensor. The catalyst is loaded into a glass cell of appropriate size, the cell is closed with airtight screws and connected to the montage by securing it in the oven, introducing the temperature sensor for the catalyst bed and connecting the gas inlet and outlet tubes.

Before starting the temperature program, the cell is purged with argon. At the end, after the final argon purge, the cell is put under vacuum and it is sealed so that the sulphided catalyst is stored in a glass ampule consequently under vacuum.

3.2.4.1 Sulphidation at 350°C

The sulphidation at 350°C follows the scheme of Figure 17. The catalyst stays 2 hours at 350°C. Then the temperature decreases to 250°C, at this point the gas is switched to argon to evacuate the H_2S which is physisorbed.

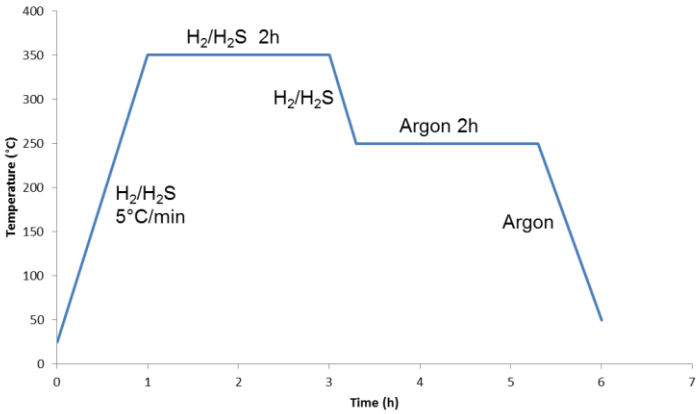

Figure 17 - Temperature and gas program for sulphidation at 350°C.

3.2.4.2 Sulphidation at room temperature

For the sulphidation at room temperature (RT) the H_2/H_2S mixture is used for 2h and then the gas is switched to argon for another 2h. The temperature is not controlled, being approximately 23-25°C with a peak at 26-28°C in the beginning of the sulphidation given that it is an exothermic process.

3.3 Catalytic test

The catalyst's performance was evaluated by the model reaction of toluene hydrogenation (HYD) in Avantium's 16 fixed bed reactor unit *Flowrence*.

The test takes place at 60 bar in gaseous phase. The catalyst is sulphided *in situ* and the same feedstock is used for the sulphidation and reaction stages.

The feed is composed of dimethyl disulphide (5,88%(w/w)), toluene (20%(w/w)) and cyclohexane (74,12%(w/w)). The sulphidation stage starts at room temperature with heating at 2°C/min up to 350°C with a plateau of at least 20 minutes and up to 120 minutes and the liquid hourly space velocity (LHSV) is $4h^{-1}$. For the catalytic test, also at 350°C, the LHSV changes to $2h^{-1}$. The reaction products are analysed by gas chromatography (GC) and 6 samples taken with 45 minute intervals. The H_2/HC ratio is constant for the two stages and equal to 450 L/L.

The toluene conversion is calculated considering all products resulting from hydrogenation of toluene and further isomerization and cracking using the average of the GC results of the two last samples taken. The relative error of the test is ±10%. The results are interpreted using a calculated intrinsic HYD rate.

The intrinsic HYD rate, in converted toluene molecules per Mo atom per hour, is given by Equation 4:

$$vHYD = \%HYD_{converted\ toluene} \times \frac{toluene\ feed\ molecules}{h} \times \frac{1}{Mo\ atoms} \quad \text{Equation 4}$$

The number of toluene molecules per hour is given by the feed stock composition and flow. The number of Mo atoms in the reactor is given by the quantity of catalyst loaded (0,45 mL) corrected by the LOI of the catalyst, its metal loading in $\%MoO_3$ and the Packing density (PD). The metal loading used in the calculations is the theoretical value obtained using the mass of metal precursor used in the

respective solution. The relative error of the PD is ±3%. The toluene conversion for each product can be consulted in Annex 4.

Equation 5 calculates the mass of MoO_3 that should be in the reactor, even if no actual MoO_3 is present, which is converted to Mo atoms by the molar mass of MoO_3 and Avogrado's Number.

$$massMoO_3(g) = \frac{\%MoO_3(\frac{w}{w_{cata}})}{100\%} \times \frac{100\% - LOI(\%)}{100\%} \times PD\left(\frac{g}{mL}\right) \times Loaded\ catalyst\ volume\ (mL) \quad \text{Equation 5}$$

3.4 Characterization Methods

All the analyses were performed by the IFPEN Physics and Analysis Division, with the exception of Raman Spectroscopy.

3.4.1 Nitrogen Physisorption

Nitrogen Physisorption (N_2 Phys.) is a textural analysis method that is based on the physical adsorption of N_2 at normal boiling point (77K) on the surface of the sample. It can be used to assess micro (d_{pore}<2 nm) and mesoporosity (2<d_{pore}<50 nm) and surface areas superior to 1m^2/g.

Not only the adsorption isotherm but also the value for Surface BET (Brunauer-Emmett-Teller) is used in this work to characterize the samples. This parameter is obtained by applying the BET equation to the points in the relative pressure (P/P_0) interval of 0,05 to 0,15. The observation of the t-curve allowed for a qualitative assessment of the microporosity.

Another parameter taken into consideration is the volume at maximum P/P_0 (which is virtually 1) that is considered to be the total pore volume of the pores up to 50 nm in diameter.

The equipment used was Micromeritics ASAP 2420. The samples go through a thermal pre-treatment at 110°C for boehmite or at 350°C for alumina.

3.4.2 Mercury Porosimetry

Mercury Porosimetry (Hg Poro.) is another textural analysis, often used in addition to N_2 Phys., and is based on the behaviour of non-wetting liquids, like mercury, that require pressure to be applied in order to penetrate a pore. This pressure is related with the pore diameter, when the pore is assumed to have a circular cross section. This analysis can evaluate pore size from 3,7 to 7000 nm (values superior to this are attributed to rugosity or powder compaction).

The pore size distribution presented in this work is the derivative of the injected volume in function of the diameter logarithm plotted in function of the diameter (dV/dlogD vs D).

Other parameters used for sample characterization are calculated as follows. The mesoporous volume (V_{meso}) is given by the difference between the injected volume at 3,7 nm and at 50 nm. The macroporous volume (V_{macro}) is calculated as the difference between the injected volume at 50nm and at 7000 nm. These volumes are especially important when there is macroporosity, which is not assessed by the Nitrogen Physisorption. Also, even for mesoporous samples, it is interesting to have a measurement from both techniques, since they are not always consistent, which is a known difficulty for researchers.

The diameter at half of the mesoporous volume ($D(V_{meso}/2)$) is used as an average diameter representative value and is the diameter correspondent to $V_{meso}/2$.

The analysis were performed in a Micromeritics Autopore IV equipment and the samples are preheated for at least 3 h at 250°C.

3.4.3 X-ray Fluorescence Spectrometry

X-ray Fluorescence Spectrometry (FX) is an elemental analysis technique that can be applied to solids, powders and liquids. The principle behind it is that when an atom is excited by an x-ray, an electron will be expelled creating a vacancy that is filled by another electron of a higher energy level, releasing energy in the form of x-rays, with this phenomenon being called fluorescence. The energy of the emitted x-rays is characteristic for each element, allowing for its identification, and the intensity of the measured peak permits quantification.

FX was used to confirm the presence of certain contaminants in the supports/catalysts prepared and the metal loading of the catalysts. The semi-quantitative analysis was performed, in which different elements can be quantified in varying matrices, but with an error of ±20% given that the various interferences are corrected by the software in a general way and a two-point only calibration curve is used. So the results are interpreted as indicative. The equipment used was a Perform'X from Thermofisher.

3.4.4 Raman Spectroscopy

Raman is a vibrational spectroscopy in which the active vibrational modes for a certain species are those that change its polarizability (indicator of the ease with which the electron cloud of a molecule can be distorted). The analysis is based on the inelastic scattering of light called Raman-Stokes scattering. This method can be applied to solids (powder, pellets, etc.), liquids and gases. It is practical for aqueous solution and supported catalyst analysis since water and alumina have no signal, allowing for simpler interpretation.

The vast majority of photons are elastically scattered when light hits a material, meaning that the scattered photons have the same energy (and thus frequency and wavelength) as the incident photons, this being known as Rayleight scattering. In this case a photon will excite an electron to a higher energy state, a virtual state, and then the electron will decay to the starting vibrational level emitting a photon with the same energy as the incident photon.

A small fraction of light can be inelasticly scattered. In this case, the electron is excited to the virtual state and decays to a level different from the starting one, meaning that the emitted electron will have an energy distinct from the incident photon. When the electron starting level is the fundamental state the scattered photon will have a lower energy than the incident photon, and this is called Raman-Stokes scattering. When the electron starting level is a higher energy vibrational level and after excitation it decays to a level of lower energy than the initial one it is called Anti-Stokes scattering, with the scattered photon being more energetic than the incident photon. The Raman-Stokes scattering is much more likely to occur that the Anti-Stokes Scattering.

The Raman shift (difference between the wavenumber of incident and scattered photons) of a set of peaks will be characteristic of certain species.

This analysis was used to identify the nature of the molybdenum species present in the prepared catalysts and in the metal solutions used. The equipment used was a Renishaw inVia Raman Microscope. The LabRAM Aramis from Horiba Scientific was used for some solutions which are later indicated. For both equipment a 532 nm wavelength laser was used.

In any case the analysis starts by confirming that the reference spectre of Si is correctly obtained. A microscope is used to focus the laser correctly on the sample surface. Then, for each sample, various spectrum with increasing laser potency are launched to assess the maximum potency that can be used, this being noted by decomposition of the material with deformation of the peaks or actual burning of the sample, visible in the microscope.

For catalysts, for each sample, two different extrudates were analysed with three spectra being obtained in distinct points for each. These were two points in the centre and one point on the edge of the extrudate, as illustrated in Figure 18.

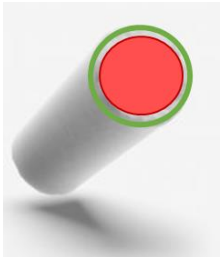

Figure 18 - Illustration of the cross section of an extrudate for which two spectra were obtained for the central area in red and one spectrum was obtained for the edge in green.

The samples are prepared by breaking an extrudate with a scalpel in one hit, not cutting with the blade to avoid changes due to local heating by friction. The extrudate is set on a support with the cut cross section facing upward.

For solutions, the liquid is placed in a sample carrier, covered with a glass lamella and the laser is focused on the liquid.

3.4.5 Thermogravimetric Analysis/Differential Thermal Analysis – Mass Spectrometry/Infrared Spectroscopy

Thermogravimetric Analysis (TG) measures the mass change of a sample in function of the temperature and Differential Thermal Analysis (DTA) measures the temperature difference between the sample and an inert reference. The compounds released during the heating of the sample can be identified by Mass Spectrometry (MS) and/or Infrared Spectroscopy (IR).

The analyses were performed under a flow of air of 25 mL/min with heating from 25°C to 700°C at a rate of 5°C/min. For TG/DTA(-IR) a TGA-DSC1 Mettler thermoscale was used and for TG-MS a TGA 851 Mettler thermoscale and Thermostar/Pfeiffer mass spectrometer were used.

3.4.6 Powder X-ray Diffraction

X-ray Diffraction (XRD) is a technique used for phase identification of crystalline materials based on the diffraction of x-rays by those materials, following Bragg's Law.

The analysis was used to quantify the boehmite in catalysts sulphided at 350°C and to identify the presence of MoS_2. To quantify the boehmite, mixtures of 50% of the sample and 50% of an internal standard (α-Al_2O_3) were analysed. The samples are ground into powder and compacted in a sample carrier. The equipment used was a PANalytical X'Pert Pro diffractometer.

3.4.7 X-ray Photoelectron Spectroscopy

X-ray Photoelectron Spectroscopy (XPS) is a surface analysis technique based on the photoelectric effect. The sample is exposed to x-rays that cause photoelectrons to be emitted by the surface that have a kinetic energy characteristic of the source element and its chemical state. A maximum depth of 5-10 nm can be analysed.

This technique was used to measure the relative quantity of sulphided Mo in the catalysts that have undergone cell sulphidation to assess its success. The equipment used was an Esca Kratos Axis Ultra spectrometer.

3.4.8 Electron Probe Microanalyser

The Electron Probe Microanalyser (EPMA) is a tool to determine the chemical composition of small solid samples without destruction. The sample is bombarded with a focused and accelerated electron beam that causes the emission of x-rays, heat and electrons, allowing for imaging and composition determination.

This analysis was used to evaluate the presence of certain elements on the cross section of one calcined catalyst. The equipment used was a Microsonde JEOL 8800R.

.

(This page was intentionally left in blank)

4. Results and Discussion

4.1 Catalyst Set 1

Catalyst Set 1 groups the catalysts prepared according to the first strategy employed of co-mixing ammonium heptamolybdate and molybdenum oxide with phosphoric acid in a conventional mixing protocol. A catalyst prepared by impregnation was prepared to serve as reference in the catalytic testing.

With this set the aim is to compare the introduction of metal precursor by co-mixing with the classical method of impregnation. The use of heptamolybdate is based on the fact that it was one of the first widely used Mo precursors. The molybdenum oxide with phosphoric acid is a more modern Mo precursor and, in the P/Mo ratio used, should form in solution a Strandberg type HPA, $P_2Mo_5O_{23}^{6-}$.

It should be noted that the catalysts that went into testing are the dried ones, as shown in section 3.1.1. This way the support is still boehmite, since there was no calcination prior to the use in the reactor. Despite boehmite not being the support material for any industrial catalysts, given that it is not thermally stable, it was used in this case to avoid performing a calcination on the Mo-containing extrudates. The work was done on the premise that upon calcination there could be sintering of the metal and/or the formation of other Mo oxides that are stable and difficult to sulphide. A fraction of the extrudates was calcined only for analysis proposes.

4.1.1 Textural properties

The textural properties of the dried, sulphided and calcined extrudates were evaluated by N_2 Phys. and Hg Poro. All the considered parameters for Catalyst Set 1 products can be consulted in Annex 2 and the parameters of the reference supports can be consulted in Annex 3.

4.1.1.1 Comparison with support

The catalysts prepared by co-mixing were compared to supports prepared in the same mixing conditions. These are an acid mixing stage followed by a neutralization by mixing with an ammonia solution.

For this comparison the analysis results of calcined extrudates were used, so that the same material, alumina, is compared.

4.1.1.1.1 Pural SB3

An alumina support prepared by conventional mixing with Pural SB3 but calcined at 700°C for 2h is presented here for comparison. The results are summarized in Table 3 and Figure 19.

Table 3 - Textural parameters of the support and calcined co-mixing catalysts prepared with Pural SB3

	Support Pural SB3 Conv	**Mo_7+Pural SB3 Conv**	**MoP+Pural SB3 Conv**
Calcination Temp. (°C)	700	540	540
D(V_{meso}/2) (nm)	10,37	10,20	8,41
V_{meso} (mL/g)	0,66	0,53	0,48
V_{macro} (mL/g)	0,01	0,01	0
V at P/P_0 max (mL/g)	0,743	0,607	0,548
Surface BET (m^2/g)	225	296	301

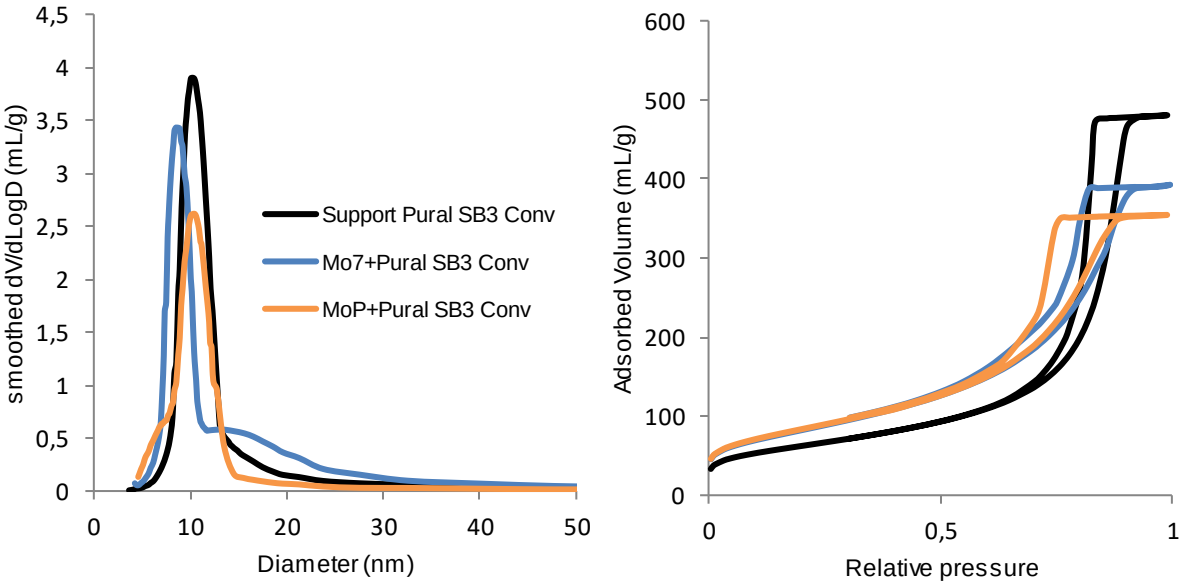

Figure 19 - Pore size distribution in the mesoporous zone obtained by Hg Poro. (left) and adsorption isotherms obtained by N_2 Phys. (right) for Pural SB3 support and catalysts

Firstly, the surface area of the support is lower than the surface area of the co-mixing catalysts. This is attributed to two main reasons: on the one hand the support was calcined at higher temperature and on the other hand the presence of Mo has shown to lead to an increase in surface area. [30] The Surface BET of the two co-mixing products can be considered essentially equal, considering that the measurement error is typically around ±10m^2/g.

Second, there is clearly a decrease in pore volume for the co-mixing catalysts. The isotherms and V at P/P_0 max show that, with MoP+Pural SB3 Conv having the lowest pore volume. In all cases there is no macroporosity.

Third, it was found that for the co-mixing catalyst with heptamolybdate the maximum of the Pore Size Distribution (PSD) is at a pore diameter of 9 nm, but the existence of some porosity for diameters superior to 10 nm cause the average diameter D(V_{meso}/2) to be superior to 9 nm. For the co-mixing product with MoO_3 and H_3PO_4 the PSD maximum is at a pore diameter of 10 nm, however the volume at diameters inferior to 10 nm cause a decrease in D(V_{meso}/2).

Nevertheless, co-mixing products show a set of textural properties adequate for use in HDT. The similarities of their PSD compared to the support suggest that an efficient peptization was accomplished. The major difference lays in a decrease of pore volume.

4.1.1.1.2 Powder X

An alumina support prepared with Powder X by conventional mixing is used as reference for the Powder X co-mixing catalysts. Table 4 and Figure 20 resume the results.

Table 4 - Textural parameters of the support and conventional co-mixing catalysts prepared with Powder X

	Support Powder X Conv	**Mo_7+Powder X Conv**	**MoP+Powder X Conv**
Calcination Temp. (°C)	540	540	540
D(V_{meso}/2) (nm)	11,15	10,79	10,10
V_{meso} (mL/g)	0,77	0,67	0,64
V_{macro} (mL/g)	0,02	0,01	0
V at P/P_0 max (mL/g)	-	0,752	0,731
Surface BET (m^2/g)	291	334	329

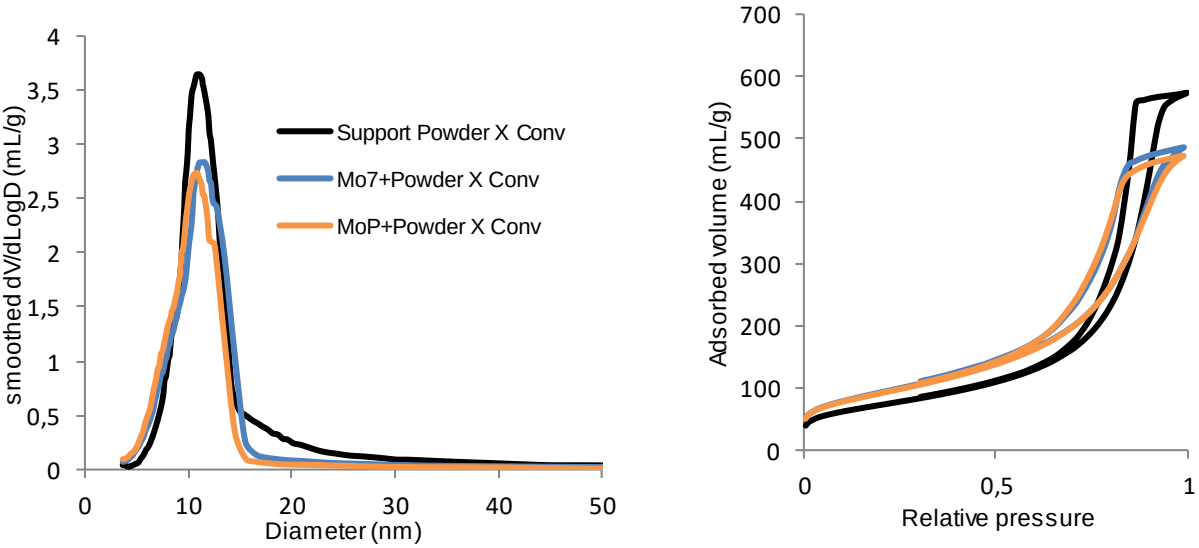

Figure 20 - Pore size distribution in the mesoporous zone obtained by Hg Poro. (left) and adsorption isotherms obtained by N_2 Phys. (right) for Powder X support and catalysts

To begin with, there is an increase in surface area of the co-mixing products in relation to the support. As mentioned above, this result is supported by other work, in which it was also found that there is an increase in surface area when molybdenum species are present. That effect was explained by the formation of slit shaped pores and by inhibition of alumina sintering during calcination by the molybdenum. [30] The surface area of the two co-mixing catalysts is the same within the measurement error.

In second place, there is again a decrease in pore volume for the co-mixing products, clearly shown in Figure 20, and no macroporosity.

Moreover, in this case the average pore diameter is essentially the same and around 10 nm for all products, as the PSD indicates.

To conclude, the co-mixing products show appropriate textural properties, an effective peptization took place and a decrease in pore volume is observed for co-mixing as well as an increase in surface area.

In comparison to Pural SB3 products, Powder X have overall a higher pore diameter and pore volume. There is also a difference in the shape of the isotherm, with a tilt on what would be called the plateau. This can be associated with the shape and interconnection of the pores being different depending on the alumina precursor used.

4.1.1.2 Comparison of dried, sulphided and calcined catalysts

The textural parameters of calcined extrudates were presented, however the dried catalysts are the solids that were tested. Thus, this section is dedicated to the parameters of the dried extrudates. These will be compared to the extrudates sulphided at 350°C and to the calcined extrudates to check the evolution upon heating.

For each boehmite powder the results of co-mixing with heptamolybdate will be shown, to provide a cleared reading, given that the final conclusions are the same for the catalyst prepared by co-mixing with molybdenum trioxide and phosphoric acid. There should be some caution when analysing this results given that at each stage the material will be different: the dried catalyst is boehmite, the sulphided one a mixture of boehmite and alumina (see section 4.1.3) and the calcined catalyst is alumina.

4.1.1.2.1 Pural SB3

The textural parameters for dried, sulphided and calcined Mo_7+Pural SB3 Conv are presented in Table 5 and Figure 21.

Table 5 - Textural parameters for dried, sulphided and calcined Mo_7+Pural SB3 Conv

Mo_7+Pural SB3 Conv	*Dried*	*Sulphided*	*Calcined*
Treatment Temp. (°C)	80	350	540
D(V_{meso}/2) (nm)	8,01	9,78	10,20
V_{meso} (mL/g)	0,45	0,46	0,53
V_{macro} (mL/g)	0,01	0	0,01
V at P/P_0 max (mL/g)	0,472	0,502	0,607
Surface BET (m^2/g)	259	230	296

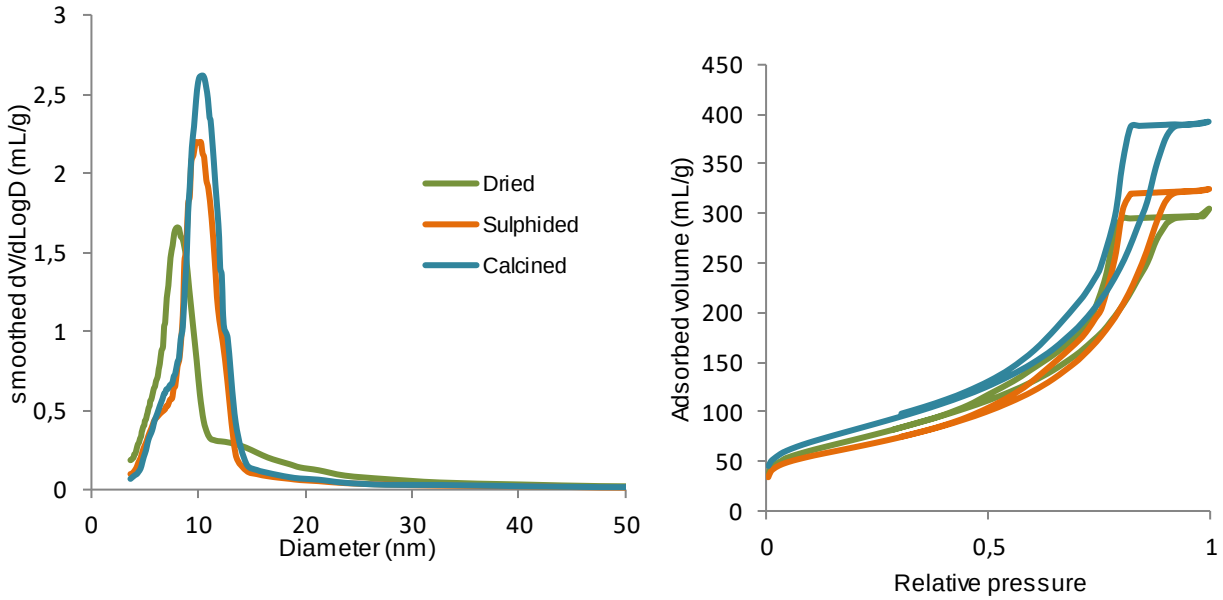

Figure 21 - Pore size distribution in the mesoporous zone obtained by Hg Poro. (left) and adsorption isotherms obtained by N2 Phys. (right) for Mo_7+Pural SB3 Conv

An increase of the temperature of the applied treatment increases the average pore diameter and pore volume. The increase in pore diameter of the calcined extrudates in comparison with the dried ones in the mesoporous range is consistent with the observations of Minoux [30].

The sulphided extrudates, receiving a thermal treatment in-between drying and calcination, present intermediate properties and should be the most representative of the catalyst that undergone reaction in the catalytic testing (since there is *in situ* sulphidation at 350°C prior to the reaction).

4.1.1.2.2 Powder X

The textural parameters for dried, sulphided and calcined Mo_7+Powder X Conv are presented in Table 6 and Figure 22.

Table 6 - Textural parameters for dried, sulphided and calcined Mo_7+Powder X Conv

Mo_7+Powder X Conv	*Dried*	*Sulphided*	*Calcined*
Treatment Temp. (°C)	80	350	540
D(V_{meso}/2) (nm)	9,27	10,63	10,79
V_{meso} (mL/g)	0,56	0,56	0,67
V_{macro} (mL/g)	0,01	0,01	0,01
V at P/P_0 max (mL/g)	0,578	0,646	0,752
Surface BET (m^2/g)	294	270	334

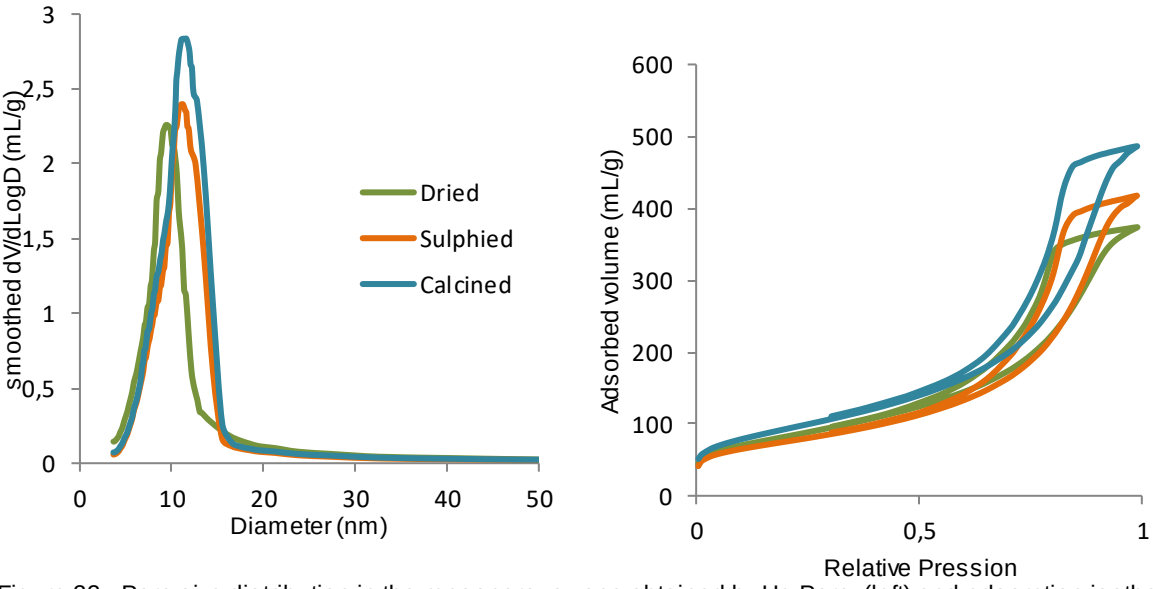

Figure 22 - Pore size distribution in the mesoporous zone obtained by Hg Poro. (left) and adsorption isotherms obtained by N_2 Phys. (right) for Mo_7+Powder X Conv

In the same way, the pore volume and average diameter increase from the dried to the calcined catalysts, with the sulphided extrudates being intermediate. An increase in surface area is observed for the calcined product.

It was mentioned in section 2.2 that higher calcination temperatures usually led to lower surface area. Be that as it may, that behaviour is not observed here nor was it for the Pural SB3 co-mixing products. In these two cases there is boehmite in the dried extrudates and a mixture of boehmite and alumina in the sulphided extrudates, so these two thermal treatments are not calcinations. Thus the relationship between subjected temperature and surface BET may not the one indicated in section 2.2.

4.1.2 Mechanical Properties

No analysis were performed on the dried catalysts which were tested. However it can be said from observation that the dried extrudates were resistant to handling, to the cell sulphidation and finally also to the catalytic test.

4.1.3 XRD on sulphided extrudates

As mentioned above, the sulphided (350°C) catalysts are composed of a mixture of boehmite and alumina and were analysed by XRD to quantify the quantity of these two phases. The XRD analysis on these extrudates show the presence of boehmite, γ-Al_2O_3 and MoS_2. The quantity of boehmite in each sulphided catalyst is indicated in Table 7. The diagrams obtained are presented in Annex 7.

Table 7 - Quantity of boehmite in the sulphided extrudates of each catalyst given by XRD

	Boehmite %(w/w)
Mo_7+Pural SB3 Conv	33
MoP+Pural SB3 Conv	35
Mo_7+Powder X Conv	17
MoP+Powder X Conv	18

It is clear that, for the same temperature program during sulphidation, the quantity of boehmite in the Pural SB3 extrudates is almost double of the quantity in the Powder X products. It shows in yet another way that different starting boehmite powders will produce distinct products. There is a relationship between crystallite size and starting temperature of boehmite to alumina transition which may explain this result. [31]

4.1.4 FX results

The composition of the dried catalysts prepared by co-mixing was determined by FX to verify the metal loading. The method used was a semi-quantitative one with a large error associated since a two point calibration curve is used and the interferences inherent to the technique are averagely corrected. Thus the results are taken as indicative.

So, the products present a metal loading in the range of 10% MoO_3 (and 2% P_2O_5 when applicable). The results can be consulted in Annex 5.

4.1.5 Assessment of present species by Raman Spectroscopy

The nature of the molybdenum species actually present in the catalysts produced and solutions used was determined by Raman Spectroscopy. For each case a spectrum for the interior and the edge of the same extrudate will be presented, for clarity of the analysis.

4.1.5.1 Metal Precursor Solutions

The metal precursor solutions representative of those used for the co-mixing were prepared for analysis with a molybdenum concentration of approximately 0,8 M. Since for co-mixing with Pural SB3 the nitric acid is added to the metal solutions, it was also added to the analysed solutions. These spectra were obtained on the LabRAM Aramis equipment.

4.1.5.1.1 Heptamolybdate solutions

The spectra of the heptamolybdate solutions with and without nitric acid are presented in Figure 23.

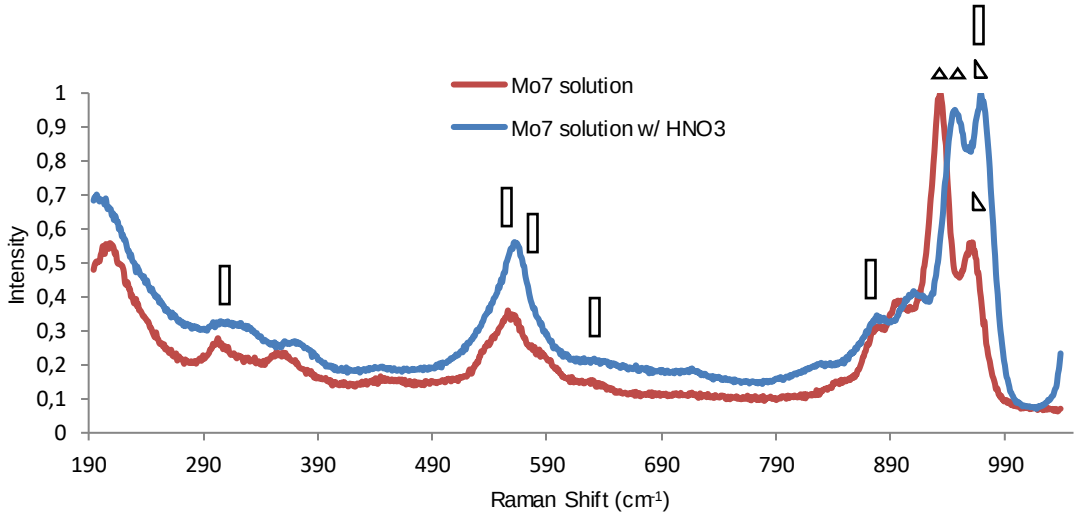

Figure 23 – Raman spectrum of the heptamolybdate solution and of the heptamolybdate solution with added nitric acid. Triangle – heptamolybdate; Rectangle triangle – octomolybdate; Rectangle-Peroxodimolybdenum

In the solution without acid mainly heptamolybdate is found at 930 cm^{-1} but also what could be octomolybdate at 960 cm^{-1}. When nitric acid is present the octomolybdate peak at 970 cm^{-1} becomes more relevant, which is in agreement with the aqueous chemistry of molybdenum that presents polymerization with pH decrease. Despite being in solution, octomolybdate is not detected in the catalysts, as shown ahead, so it is considered that the octomolybdate is transformed to heptamolybdate during the mixing by the basic hydroxyl groups of the boehmite and/or by the ammonia solution used in the neutralisation stage.

Since this solution is prepared with hydrogen peroxide, a peroxodimolybdenum species $Mo_2O_2(O_2)_4^{2-}$ also appears to be present. This compound should be more soluble in water justifying the use of the H_2O_2. It is identified by peaks at 960, 870, 626, 571, 541 and 318 cm^{-1}. The peak at 870 cm^{-1} could also be hydrogen peroxide. [32] [33] The peroxodimolybdenum is not found in the prepared catalysts, so it should decompose during the mixing and/or the drying of the extrudates.

In all, in these solutions there is a mixture of heptamolybdate, octomolybdate and peroxodimolybdenum.

4.1.5.1.2 Molybdate trioxide and phosphoric acid solutions

The spectra of the solutions with and without nitric acid are shown in Figure 24.

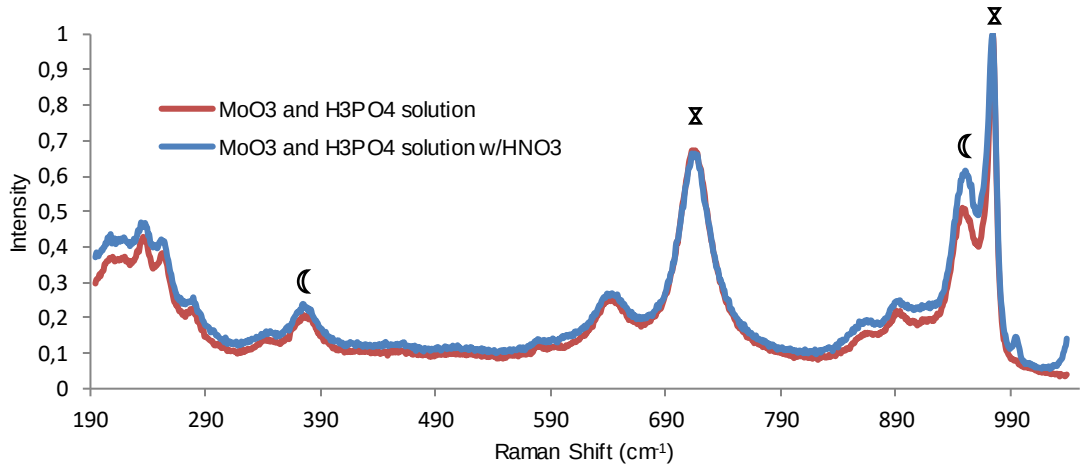

Figure 24 - Raman spectrum of the MoO_3 and H_3PO_4 solution and of the solution of the same compounds with added nitric acid. Hourglass – Dawson HPA; Crescent – Strandberg HPA

In this case there appears to be no difference in the presence of nitric acid. Two different HPAs may be identified. Peaks at 715 and 970 cm^{-1} can be attributed to Dawnson type HPA $P_2Mo_{18}O_{62}^{n-}$ whereas the Strandberg type HPA $P_2Mo_5O_{23}^{6-}$ could be recognized by the peaks at 940 and 370 cm^{-1}.

4.1.5.2 Co-mixing with Pural SB3

The spectra of the dried and calcined extrudates will be presented, as well as the spectra of the solutions used in the co-mixing.

4.1.5.2.1 Co-mixing with heptamolybdate

The spectra of the dried catalyst prepared by co-mixing with heptamolybdate is represented in Figure 25.

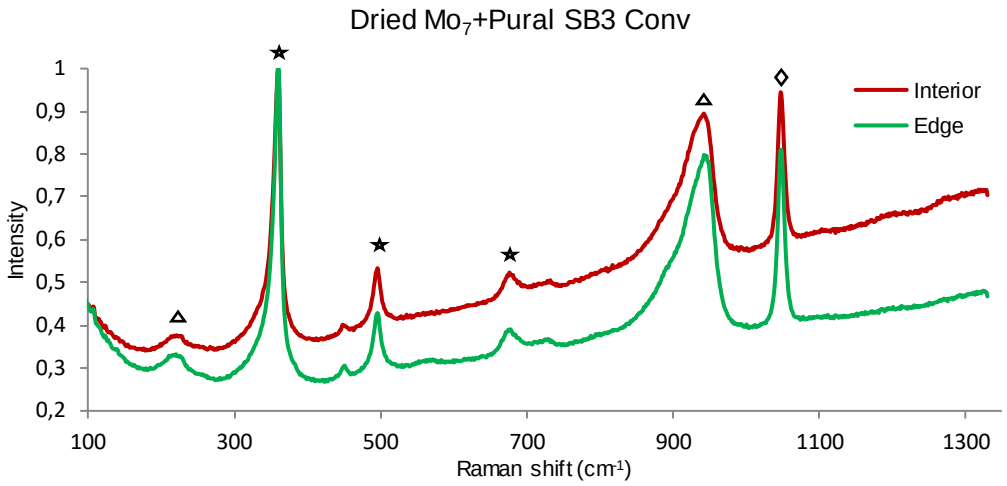

Figure 25 – Raman spectra of a point on the interior (red) and on the edge (green) of a dried Mo_7+Pural SB3 Conv extrudate. Star - boehmite; Triangle – heptamolybdate; Lozenge – Nitrate ion

The peaks characteristic of boehmite are present at 360, 450, 495 and 676 cm^{-1} [30]. The peak at 1050cm^{-1} corresponds to the nitrate ion. The presence of heptamolybdate is clear and predominant with the peaks at 940 cm^{-1} and 223 cm^{-1} [34]. A slight *shoulder* at around 900 cm^{-1} might suggest some monomolybdate, however its other identifying band at 320 cm^{-1} is not distinguishable from the intense boehmite peak.

In conclusion, the catalyst is homogeneous showing the same spectra for the interior and the edge and the main deposited species is the heptamolybdate as desired.

Figure 26 represents the spectrum of the calcined catalyst. There is a broadening of the peaks for calcined extrudates that increases the difficulty of a clear attribution.

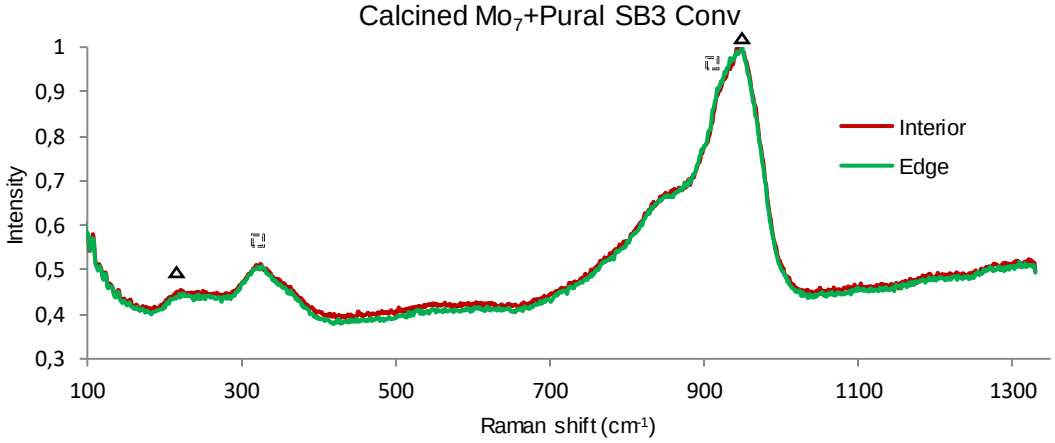

Figure 26 - Raman spectra of a point on the interior (red) and on the edge (green) of a calcined Mo7+Pural SB3 Conv extrudate. Triangle – heptamolybdate; Dotted square – monomolybdate

Since this is the calcined catalyst there are no peaks corresponding to boehmite or to the nitrate ion. Again the heptamolybdate is predominant species at 950 and 220 cm^{-1}. A shoulder at 920-930 cm^{-1} and the peak at 320 cm^{-1} could confirm the presence of monomolybdate. The wide band at 840-870

cm^{-1} should be a mixture of molybdenum species. Molybdenum trioxide is not present, since its identifying bands are at 660, 820 and 980cm^{-1}.

Altogether, heptamolybdate is still the main Mo species and the extrudates are homogeneous, with the presence of monomolybdate being possible. This might have formed due to the basic hydroxyl groups at the surface of the boehmite crystallites. The nonexistence of MoO_3 after thermal treatment opens the possibility of calcination of the extrudates, to have an alumina support, without the risk of severely damaging sulphidation ability by formation of such refractory species.

4.1.5.2.2 Co-mixing with molybdenum trioxide and phosphoric acid

The spectra of dried and calcined extrudates of molybdenum trioxide and phosphoric acid co-mixing with Pural SB3 are presented in Figure 27 and Figure 28, respectively.

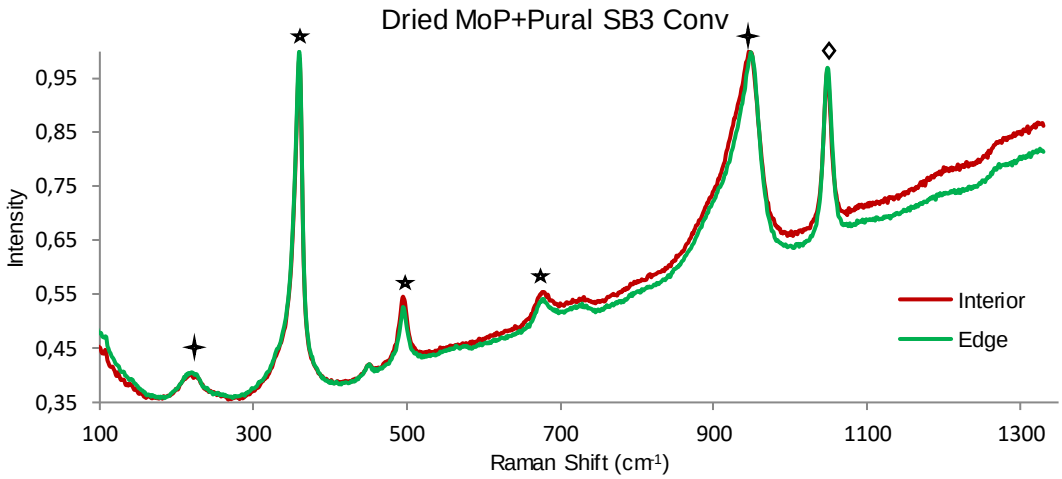

Figure 27 - Raman spectra of a point on the interior (red) and on the edge (green) of a dried MoP+Pural SB3 Conv extrudate. Lozenge – Nitrate ion; Star – boehmite; Four point star – Mo species

It is difficult to identify the molybdenum species present in the dried extrudate due to the intense boehmite peak at 360 cm^{-1}. The peaks at 950 and 220 cm^{-1} could be attributed to the Strandberg type HPA, $P_2Mo_5O_{23}^{6-}$ [34], however the other characteristic peak is at 370 cm^{-1} and it cannot be said if it is present or not due to the boehmite peak. The extrudates are homogeneous between the edge and the interior.

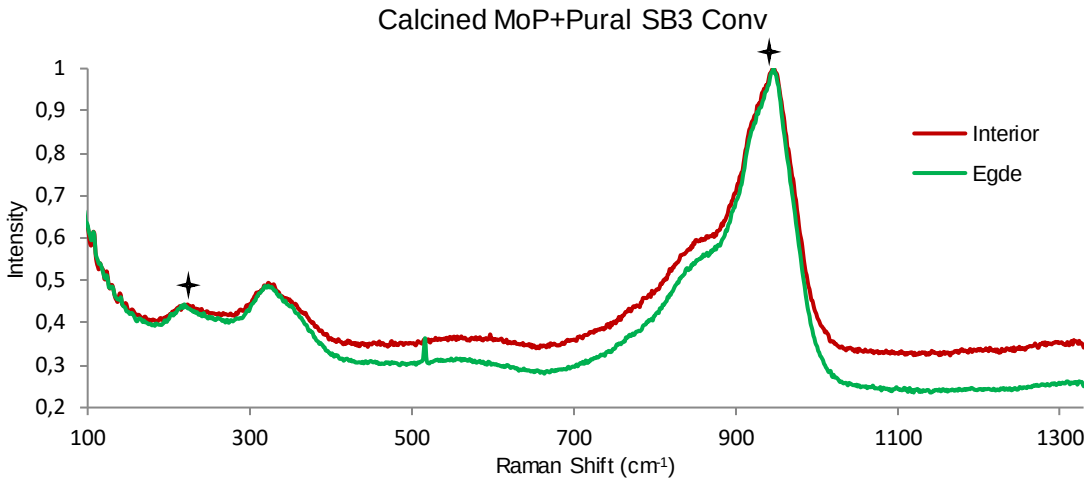

Figure 28 - Raman spectra of a point on the interior (red) and on the edge (green) of a calcined MoP+Pural SB3 Conv extrudate. Four point star – Mo species

The interpretation of the spectra of the calcined is even more difficult, although it may be said that the Strandberg type HPA could still be present considering the peaks at 220 cm^{-1} and 950 cm^{-1}. It is observed that no MoO_3 crystallites formed during calcination.

4.1.5.3 Co-mixing with Powder X

In the case of Powder X, the spectra of the dried extrudates do not give much information given that the fluorescence from the methocel is more intense than any of the peaks. Only the spectra for the calcined extrudates are discussed.

4.1.5.3.1 Co-mixing with heptamolybdate

The spectra for a calcined extrudate of catalyst prepared by co-mixing with heptamolybdate is presented in Figure 29.

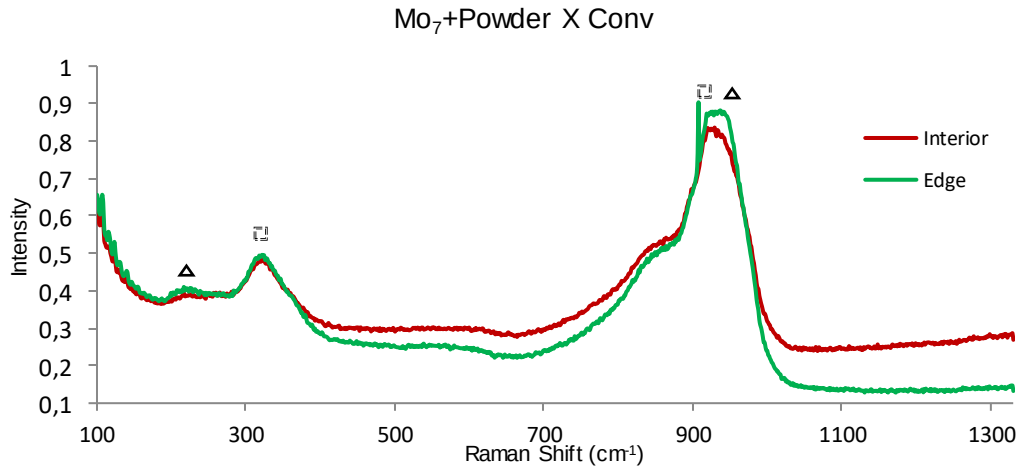

Figure 29 - Raman spectra of a point on the interior (red) and on the edge (green) of a calcined Mo_7+Powder X Conv extrudate. Triangle – heptamolybdate; Dotted square – monomolybdate

The band at 920-950 cm^{-1} may be attributed to a mixture of monomolybdate and heptamolybdate, supported by the peaks at 320 and 220 cm^{-1} respectively. Again a broad band of mixed Mo oxides appears at 820-870 cm^{-1}.

The conclusions are the same as in section 4.1.5.2.1: possible presence of both mono and heptamolybdate, homogeneity between edge and interior and finally MoO_3 was not found.

4.1.5.3.2 Co-mixing with molybdenum trioxide and phosphoric acid

The spectra for a calcined extrudate of catalyst prepared by co-mixing with molybdenum trioxide and phosphoric acid is presented in Figure 30.

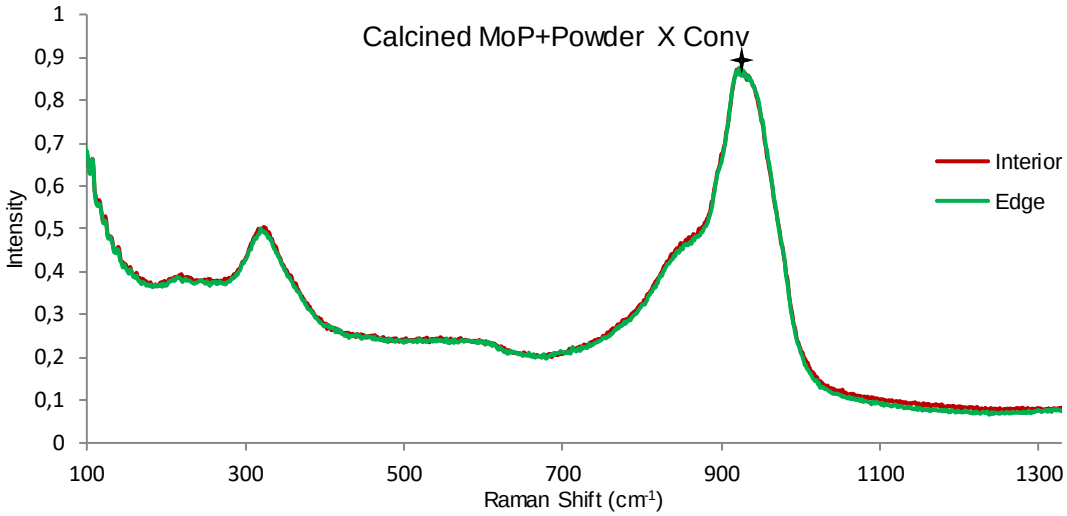

Figure 30 - Raman spectra of a point on the interior (red) and on the edge (green) of a calcined MoP+Powder X Conv extrudate. Four point star – Mo species

Once more the spectra are of difficult interpretation, but it seems molybdate in strong interaction with the support is found, given that there is a peak at 920 cm^{-1} and no clear band at 220 cm^{-1}. Nevertheless it there is once more no formation of MoO_3.

4.1.5.4 Impregnation of heptamolybdate over a Powder X support

The spectra of Mo_7/Powder X Conv are presented in Figure 31. This is the catalyst prepared by impregnation to be used as reference, and after the metal deposition it undergoes maturation and drying only.

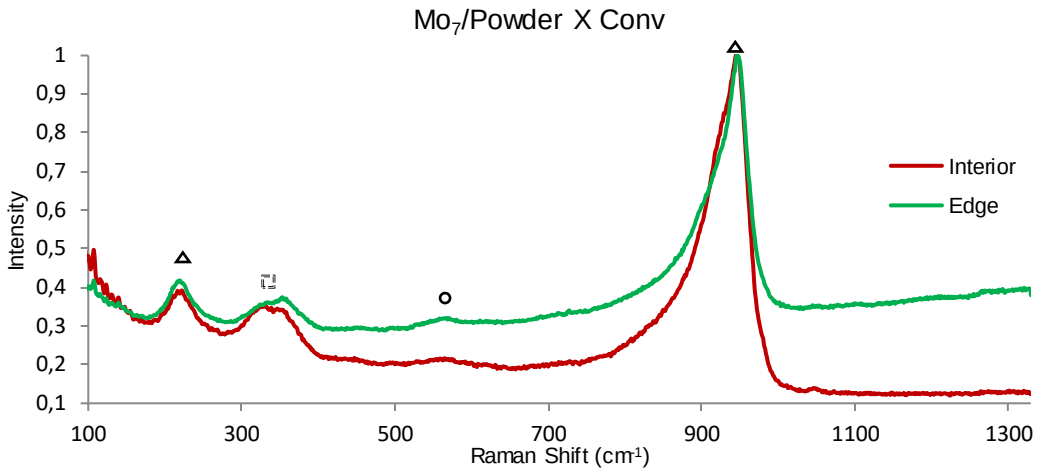

Figure 31 - Raman spectra of a point on the interior (red) and on the edge (green) of Mo_7/Powder X Conv. Triangle – heptamolybdate; Dotted square – monomolybdate; Circle - Anderson (Al) HPA

Heptamolybdate is the main species; with the peaks at 950 and 220 cm^{-1}. The peak at 330 cm^{-1} indicates the presence of monomolybdate. The small band at 570 cm^{-1} is attributed to the aluminium Anderson HPA, $AlMo_6O_{24}H_6^{3-}$. The HPA also contributes to the peak at 950 cm^{-1}.

This is characteristic of a catalyst prepared by impregnation, as described in section 2.1.4.1.1, and the homogeneity between interior and edge show that the process was adequately performed.

4.1.6 XPS results

The catalyst prepared by co-mixing of molybdenum trioxide and phosphoric acid with Powder X (MoP+Powder X Conv) was sulphided at 350°C and was analysed by XPS. Only one sample was tested due to the availability of the analysis equipment. The result of 80% of sulphided Mo in relation to the total Mo is in the normal range of sulphidation in the conditions used.

It can be concluded that the possible trapping of Mo precursor in the walls of the catalyst, if existing, is not significant. The possible difference between the interaction of the metal precursor with the support in co-mixing products relative to classic catalysts, if existent, also appears to have no effect on the sulphidation rate.

4.1.7 Catalytic test results

The intrinsic hydrogenation rate resulting from the toluene hydrogenation test for the catalysts of Set 1 is given in Figure 32. The relative error of the presented rate was obtained by error propagation (exemplified in Annex 6) considering that the toluene conversion (Annex 4) has a relative error of ±10% and the Packing Density of ±3%. The values are shown with the number of significant figures given by that calculated error.

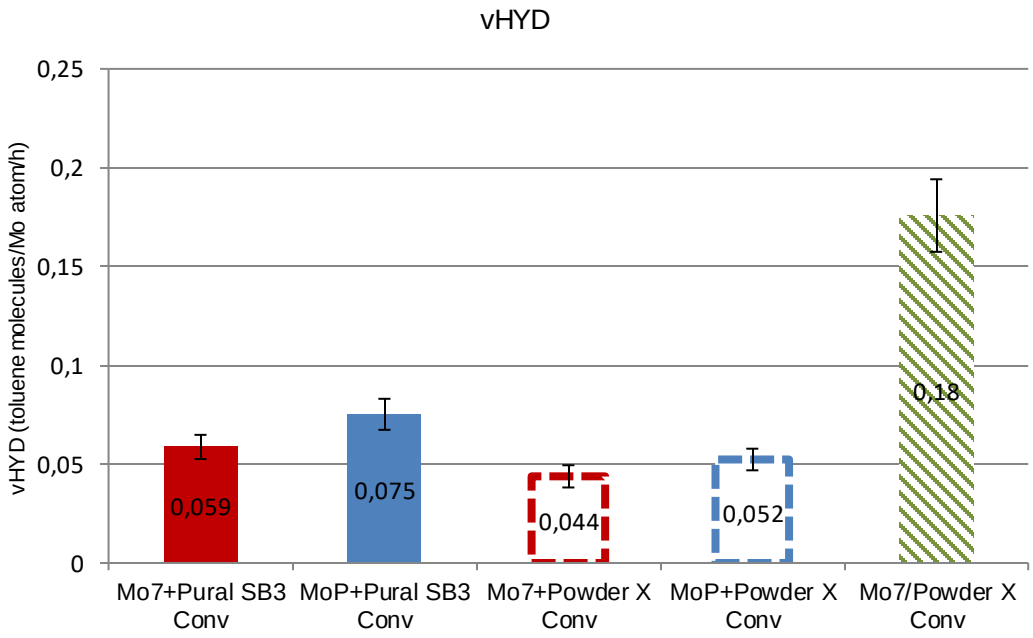

Figure 32 – Histogram of the intrinsic hydrogenation rate for the catalysts of Set 1

First, for the co-mixing products, there is a slight increase in activity when MoP is used in comparison to the heptamolybdate. This was expected and can be attributed to the known fact that phosphorus enhances the activity of HDT catalysts. [15] Furthermore, for the same metal precursor used, Pural SB3 shows better results than Powder X, but again there is only a minor difference. The reader should keep in mind that these are catalysts in which the support material is boehmite.

Secondly, the reference catalyst prepared by impregnation has an activity of more than double than that of the co-mixing catalysts.

Therefore it is clear that the preparation of HDT catalysts by co-mixing of heptamolybdate and molybdenum trioxide and phosphoric acid with the boehmite powders used in conventional mixing conditions is not competitive with catalysts prepared by the traditional protocol.

With the information at our disposal for this set of catalysts there is no way of being sure of the cause. On the one hand there could be less Mo accessible by *trapping* of molybdenum compounds in the "walls" during co-mixing, though this idea was dismissed by the XPS results. It can be also thought that some degree of sintering may occur during drying creating large Mo clusters that later sulphide forming big MoS_2 slabs, with a smaller *active site/slab* ratio.

On the other hand, using boehmite as the support material may impact the reaction conditions. To begin with, the surface of a boehmite support is different from an alumina one, having more hydroxyl groups, which may influence not only the formation of the MoS_2 slabs and their interaction with the support (remember the difference between Type I and Type II CoMoS) but also the adsorption of reactants and products.

In second place, it was seen that the transition to alumina will start at 350°C during cell sulphidation, so the same thing may be expected to happen for the *in situ* sulphidation. The release of water in this

transformation may cause a local dilution of the feed. In a long enough test to cause the complete transition to alumina, the observation of an activity increase at that point would confirm that the boehmite support has a negative effect on catalytic performance.

Alternatively, since no MoO_3 clusters were found by Raman Spectroscopy in the calcined extrudates, the calcined catalysts could be sulphided *in situ* and tested to clarify the impact of the support material on the activity.

4.1.8 Conclusions

Non-promoted hydrotreatment catalysts can be produced by co-mixing of heptamolybdate and of molybdate trioxide and phosphoric acid in a conventional mixing protocol comprising an acid mixing stage and neutralisation.

In comparison with alumina supports, the catalysts have higher surface area, result consistent with other work [30], and lower pore volume. Being mesoporous solids, the catalysts have appropriate texture for most HDT applications.

The co-mixing products have the same species on the inside and on the edge of the extrudates, being homogenous in that sense, and clusters of MoO_3 are not found in the calcined extrudates. This provides the opportunity of calcination after co-mixing without the formation of that refractory species that is difficult to sulphide.

Regarding the catalysts' performance concerning toluene hydrogenation, the co-mixing ones have lower activity than the reference catalyst prepared by dry impregnation. Since the XPS analysis showed a normal sulphidation of Mo, there should be no relevant amount of inaccessible molybdenum species due to the co-mixing. Thus, this result was attributed to having boehmite as the support. Boehmite has a different surface chemistry than alumina and is not thermally stable so these factors may have an impact on catalyst performance.

4.2 Trial Supports

Seven trial supports were prepared to test the mixing in particular conditions. These products were characterized texture wise and compared with other supports. It was concluded that those particular conditions can be successfully used to produce supports with adequate texture.

4.3 Catalyst Set 2

Having succeeded in preparing extrudates by mixing in particular conditions, the same principle was applied to co-mixing a specific Mo precursor, following the second strategy. Nine catalysts were prepared by co-mixing and two others were prepared by impregnation.

The catalysts were characterized by: Hg Poro, N_2 Phys., Raman Spectroscopy, EPMA, FX, XRD, TG/DTA-SM/IR, XPS and toluene HYD catalytic test was performed. Only the XPS results and catalytic test results can be presented.

4.3.1 XPS results

XPS analyses were performed on catalysts sulphided at two temperatures, 350°C and room temperature. Due to the availability of the XPS equipment, it was necessary to select a limited number of samples for this analysis.

The catalysts sulphided at 350°C are two co-mixing products and the catalysts sulphided at room temperature are a catalyst prepared by co-mixing and the catalyst prepared by impregnation of heptamolybdate over a conventional Powder X calcined support from Set 1 (Mo_7/Powder X Conv). Here the objective is to assess if the catalyst prepared by co-mixing according to the second strategy of using a monoatomic metal precursor is better sulphided at low temperature when compared to a traditional catalyst.

For the sulphidation at high temperature the co-mixing catalysts have the same relative amount of sulphided molybdenum as the catalyst prepared by impregnation. This should indicate that no there is no substantial amount of inaccessible Mo that could be trapped due to the co-mixing technique.

In relation to the catalysts sulphided at low temperature, the catalyst prepared by co-mixing has more sulphided Mo than the traditional one. At this temperature the sulphided Mo is still not in the shape of slabs, however more sulphided Mo at low temperature opens the path for slab formation.

4.3.2 Catalytic test results

The catalytic test results, given by the intrinsic hydrogenation rate of toluene, of all catalysts of Set 2 are presented in this section.

The results for all the products of Catalyst Set 2 are presented in Figure 33. The catalysts A to I were prepared by co-mixing and the catalysts J* and K* are the references prepared by impregnation.

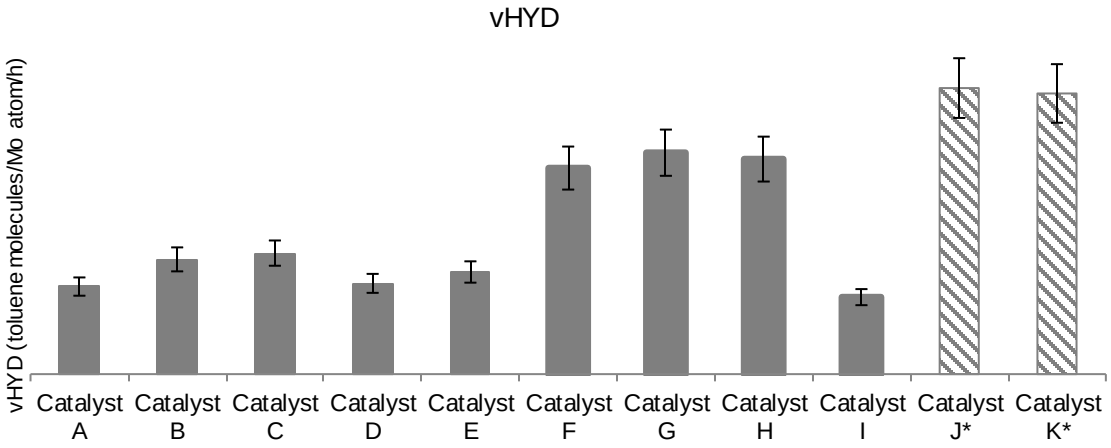

Figure 33 - Intrinsic HYD rate of toluene of all catalysts of Set 2

The co-mixing catalysts have a lower performance that the impregnation catalysts. This was attributed to the support and to a possible negative difference in the active phase of the co-mixing products.

4.4 Catalyst Set 3

The same particular mixing conditions and specific Mo precursor were employed to produce two promoted catalysts by co-mixing. A reference promoted catalyst prepared by impregnation was also synthesised.

The products were characterized by: Hg Poro., N_2 Phys., Raman Spectroscopy, FX, XPS and toluene HYD catalytic test was performed.

4.4.1 XPS results

The three catalysts of Set 3 where analysed by XPS after cell sulphidation at room temperature and after the catalytic test, where they were sulphided at 350°C and 60 bar. Unfortunately the results for spent catalysts cannot be used given that too much oxidation occurred, probably when removing the extrudates from the reactors, which was not done in a glove box.

The co-mixing catalysts have more sulphided molybdenum than the reference catalyst prepared by impregnation. After sulphidation at this low temperature the sulphided Mo is not expected to be in the form of slabs, however if the sulphidation starts at lower temperature there is more time for the sulphide phase to stabilize into slabs. If the slabs are formed earlier, then the promotion can take place easier at higher temperatures.

4.4.2 Catalytic test results

The intrinsic toluene hydrogenation rate is presented in Figure 34. Catalyst L and M were produced by co-mixing and Catalyst N* is the reference prepared by impregnation.

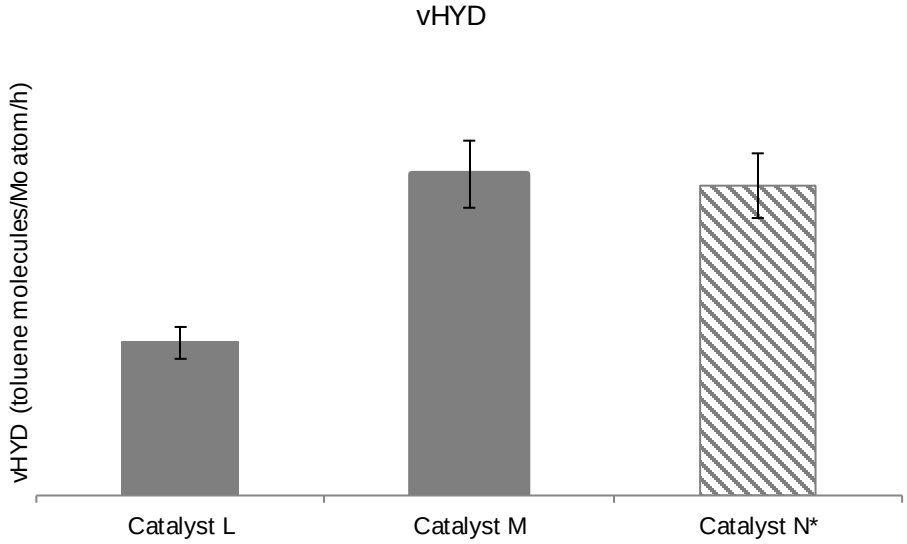

Figure 34 - Intrinsic hydrogenation rate of toluene for Catalyst Set 3 products

Catalyst M has a slightly better result, or identical considering the error, than the impregnated catalyst. This is a very positive result that shows that it is possible to produce a hydrotreatment catalyst by the simpler process of co-mixing that has the same performance as a catalyst prepared by classical impregnation.

The question remains as to why the non-promoted catalysts have worse performance than the references whereas the promoted catalyst shows the same results. It may be considered that whatever difference in the sulphided phase slabs that negatively affects the co-mixing catalysts (as hypothesised for the non-promoted ones) is overcome by a better promotion degree motivated by the higher sulphidation of Mo at low temperatures.

5. Conclusion and perspectives

5.1 Conclusion

The objective of this work was to synthesise HDT catalysts using the technique of co-mixing in order to simplify the production process and to obtain better performing catalysts.

Regarding the first strategy of co-mixing with traditional precursors, it is possible to produce non-promoted hydrotreatment catalysts by co-mixing of heptamolybdate and of molybdate trioxide and phosphoric acid in a conventional mixing protocol. These catalysts have adequate textural properties, have a uniform distribution of metallic species and present a normal degree of Mo sulphidation at high temperature. The products do not have the desired activity for toluene hydrogenation, being out performed by a traditional reference, which is mainly attributed to having boehmite as the support.

The second strategy was to use the co-mixing process in conjunction with a specific Mo precursor. For this strategy, it was firstly found that it is possible to produce supports prepared by particular mixing conditions that have textural properties in the range of those needed or HDT catalysts.

Secondly, the same mixing conditions can be applied to the co-mixing with the specific Mo precursor. The catalysts' performance in toluene HYD is still lower than the references'. Despite not having the desired performance, the co-mixing products have a normal degree of Mo sulphidation at high temperature and a better Mo sulphidation at low temperature.

Finally, the co-mixing of the same specific Mo precursor and a promoter metal precursor to produce promoted catalysts originated in one catalyst which has the same performance in toluene HYD as a classical promoted catalyst. This means that the same performance was achieved using a simplified process that takes less time and has less steps. Also, the combination of the procedures of co-mixing and impregnation open the opportunity for higher metal loadings. The co-mixing catalysts also present better sulphidation of Mo at lower temperature, which is considered to positively impact the Ni decoration of the slabs at high temperature.

5.2 Perspectives

It is believed that better results can be achieved in the future if other ideas are explored based on the results obtained in this work.

For the first strategy, testing of the calcined catalysts instead of the dried boehmite extrudates would be of interest to confirm the impact of the support material. Also, promoted catalysts should be produced by co-mixing using these Mo precursors and mixing protocol to see if another product competitive with the traditional catalysts is achieved.

The preparation of supports in the particular conditions is relatively innovative considering the divulged literature. A further and more complete study is needed to clarify this procedure. This may also lead to new protocols in support production.

In relation to the catalysts produced following the second strategy, further characterization, for example Scanning Transmission Electron Microscopy micrographs of the active phase, would be

useful to understand why the non-promoted co-mixing supports don't have the same activity as impregnated ones and why the promoted co-mixing catalyst does.

Finally, the impregnation over a co-mixing product should be tested to produce high loading catalysts, possibly avoiding the precursor solubility and re-solubilisation problems that are faced when successive impregnations are used.

Bibliography

[1] Exxon Mobil, “The Outlook for Energy: A View to 2040,” 2016.

[2] Organization of the Petroleum Exporting Countries, “World Oil Outlook,” 2015.

[3] O. a. G. Journal, “Crude demand to increase, Feed-quality changes in store,” 12 June 2010. [Online]. Available: http://www.ogj.com/articles/print/volume-108/issue-46/processing/crude-demand-to-increase-feed-quality.html. [Accessed 18 Mars 2016].

[4] H. Topsoe, B. S. Clausen and F. E. Massoth, “Hydrotreating Catalysis,” Berlin, Springer-Verlag, 1996.

[5] A. Gruia, “Hydrotreating,” in *Handbook of Petroleum Processing*, Springer.

[6] J.-F. Le Page, Applied Heterogeneous Catalysis: Design, Manufacture, and Use of Solid Catalysts, Technip.

[7] icct and Diesel Net, “EU: Light-duty: Emissions,” TransportPolicy.net, [Online]. Available: http://transportpolicy.net/index.php?title=EU:_Light-duty:_Emissions. [Accessed 23 Mars 2016].

[8] H. F. Rase, Handbook of Commercial Catalysts: Heterogeneous Catalysts, CRC Press, 2000.

[9] Axens, "Vegan," [Online]. Available: http://www.axens.net/product/technology-licensing/11008/vegan.html. [Accessed 5 April 2016].

[10] Total, "LA MÈDE: TOTAL’S FIRST BIOREFINERY," [Online]. Available: http://www.total.com/en/energy-expertise/projects/bioenergies/la-mede-total-first-biorefinery. [Accessed 5 April 2016].

[11] Markets and markets, “Refinery Catalysts Market worth $6,707.92 Million by 2019,” [Online]. Available: http://www.marketsandmarkets.com/PressReleases/global-refinery-catalyst-market.asp. [Accessed 31 Mars 2016].

[12] S. Eijsbouts, “Hydrotreating Catalysts,” in *Synthesis of solid catalysts*, WILEY-VCH, 2009, pp. 301-328.

[13] H. Topsoe, "The role of Co–Mo–S type structures in hydrotreating catalysts," *Applied Catalysis A:General,* vol. 322, pp. 3-8, 2007.

[14] F. Schüth, K. S. W. Sing and J. Weitkamp, Eds., Handbook of Porous Solids, WILEY-VCH.

[15] H. Toulhoat and P. Raybaud, Catalysis by Transition Metal Sulphides, Paris: Technip, 2013.

[16] Sebenik, Burkin, Dorfler, Laferty and Church, “Molybdenum and Molybdenum Compounds,” in *Ullmann's Encyclopedia of Industrial Chemistry*, vol. 23, Wiley-VCH, 2012, pp. 521-566.

[17] S. Eijsbouts, L. van den Oetelaar and R. van Puijenbroek, "MoS2 morphology and promoter segregation in commercial Type 2 Ni–Mo/Al2O3 and Co–Mo/Al2O3 hydroprocessing catalysts," *Journal of Catalysis,* vol. 229, pp. 352-364, 2005.

[18] Toulhoat, Raybaud, Kasztelan, Kresse and Hafner, “Transition metals to sulfur binding energies relationship to catalytic activities in HDS: back to Sabatier with first principle calculations,”

Catalysis Today, vol. 50, pp. 629-636, 1999.

[19] T. Alphazan, *Vers la conception moléculaire de catalyseurs d'hydrotraitement préparés à partir de précurseurs métallo-organiques,* Lyon, 2013.

[20] G. Busca, "Structural, Surface, and Catalytic Properties of Aluminas," in *Advances in Catalysis*, vol. 57, Elsevier, 2014, pp. 319-404.

[21] Moreaud, Jeulin, Morard and Revel, "TEM image analysis and modelling: application to boehmite nanoparticles," *Journal of microscopy,* vol. 245, pp. 186-199, 2012.

[22] Fauchadour, Kolenda, Barré and Normand, "Peptization mechanisms of boehmite used as precursors for catalysts," *Studies in Surface Science and Catalysis,* vol. 143, 2002.

[23] Trimm and Stanislaus, "THE CONTROL OF PORE SIZE IN ALUMINA CATALYST SUPPORTS: A REVIEW," *Applied Catalysis,* vol. 21, pp. 215-238, 1986.

[24] Karouia, Boualleg, Digne and Alphonse, "Control of the textural properties of nanocrystalline boehmite (γ-AlOOH) regarding its peptization ability," *Powder Technology,* vol. 237, pp. 602-609, 2013.

[25] P. Ptacek, Ed., Strontium Aluminate - Cement Fundamentals, Manufacturing, Hydration, Setting Behaviour and Applications, InTech, 2014.

[26] Kemp and Adams, "Hydrogel-derived catalysts. Laboratory results on nickel-molybdenum and cobalt-molybdenum hydrotreating catalysts," *Applied Catalysis A: General,* vol. 134, pp. 219-317, 1996.

[27] H. D. Simpson, "DESULFURIZATION PROCESS AND CATALYST". Patent US 4097413, 1978.

[28] D. W. Blakely, "METHOD FOR COMULLING METALS WITHOUT CRYSTAL FORMATION". Patent US 4402865, 1983.

[29] Armaroli, Minoux, Gautier and Euzen, "A DRIFTS study of Mo/alumina interaction: from Mo/boehmite solution to Mo/gamma-alumina," *Applied Catalusis A: General,* vol. 251, pp. 241-253, 2003.

[30] M. Delphine, "Préparation de catalyseurs d'hydrotraitement par comalaxage molybdène-boehmite : influence sur les propriétés texturales, structurales et catalytiques du matériau final.," 2002.

[31] K. Fouad, "Traitement thermique de boehmite de taille et forme de particules contrôlées : vers l'optimisation des propriétés de l'alumine gamma," 2014.

[32] Campbell, Dengel, Edwards and Griffith, "Studies on Transition Metal Peroxo Complexes. Part 8. The Nature of Peroxomolybdates and Peroxotungstates in Aqueous Solution," *J. Chem Soc. Dalton Trans,* vol. 1203, pp. 1203-1208, 1989.

[33] Rochet, Baubet, Moizan, Devers, Hugon, Pichon, Payen and Briois, "Influence of the Preparation Conditions of Oxidic NiMo/Al2O3 catalysts on the Sulfidation Ability: A Quick-XAS and Raman Spectroscopic Study," *Journal of Physical Chemistry C,* vol. 119, pp. 23928-23942, 2015.

[34] Bergwerff, Visser, Leliveld, Rossenaar, d. Jong and Weckhuysen, "Envisagin the physicochemical processes during the preparetio of supported catalysts: Raman microscopy on the impregnation of Mo onto Al2O3 extrudates," *Jounal of the American Chemical Society,* no. 126, pp. 14548-14556, 2004.

Annexes

Annex 1 – Alumina precursor powders' properties

The Loss on Ignition of the powders is determined by establishing the weight difference before and after calcination in a muffled oven at 1000°C for 3h. The sample is weighted at 250°C to avoid water physisorption after calcination.

The Packing Density of the powders is obtained by filling a measuring tube with the powder while tapping it for compaction.

Table i - LOI and PD of the used alumina precursor powders

	LOI (%)	PD (g/mL)
Pural SB3	29,4	0,92
Powder X	28,0	0,51

Annex 2 – Catalyst Set 1 products' properties

The Loss on Ignition of the catalysts is determined by establishing the weight difference before and after calcination at 500°C for 30 minutes. The samples are kept in a desiccator until cool enough to handle for weighting after calcination. The Packing Density is obtained by filling a measuring tube in six times and tapping it 400 times after each partial filling with Autotap from Quatachrome.

The textural properties and respective errors are given by Hg Poro. and N_2 Phys. The parameters indicate for the impregnation catalyst Mo_7/Powder X Conv are those of the impregnated support.

Table ii - LOI, PD and textural parameters of Catalyst Set 1 products

	Mo_7+Pural SB3 Conv	**MoP+Pural SB3 Conv**	**Mo_7+Powder X Conv**	**MoP+Powder X Conv**	**Mo_7/Powder X Conv**
LOI (%)	22,85	22,68	23,90	22,52	7,46
PD (g/mL)	0,823	0,876	0,664	0,689	0,565
	Dried extrudates				-
Treatment temp. (°C)	80				-
D(V_{meso}/2) (nm)	8,01±0,16	6,30±0,13	9,27±0,19	9,14±0,18	11,15±0,22
V_{meso} (mL/g)	0,45±0,02	0,40±0,02	0,56±0,03	0,55±0,03	0,77±0,04
V_{macro} (mL/g)	0,01±0	0±0	0,01±0	0,01±0	0,02±0
V at P/P_0 max (g/mL)	0,472±0,009	0,525±0,011	0,578±0,012	0,563±0,011	-
Surface BET (m^2/g)	259±12,95	329±16,45	294±14,70	283±14,15	262±13,10
	Sulphided extrudates				
Treatment temp. (°C)	350				
D(V_{meso}/2) (nm)	9,78±0,20	7,83±0,16	10,63±0,21	9,92±0,20	
V_{meso} (mL/g)	0,46±0,02	0,41±0,02	0,56±0,03	0,55±0,03	
V_{macro} (mL/g)	0±0	0,01±0	0,01±0	0±0	
V at P/P_0 max (g/mL)	0,502±0,010	-	0,646±0,013	0,640±0,013	
Surface BET (m^2/g)	230±11,50	-	270±13,50	274±13,70	
	Calcined extrudates				
Treatment temp. (°C)	540				
D(V_{meso}/2) (nm)	10,20±0,20	8,41±0,17	10,79±0,22	10,11±0,20	
V_{meso} (mL/g)	0,53±0,03	0,48±0,02	0,67±0,03	0,64±0,03	
V_{macro} (mL/g)	0,01±0	0±0	0,01±0	0±0	
V at P/P_0 max (g/mL)	0,607±0,012	0,548±0,011	0,752±0,015	0,731±0,015	
Surface BET (m^2/g)	296±14,80	301±15,05	334±16,70	329±16,45	

Annex 3 – Reference supports properties

Table iii - Textural parameters of reference supports. An asterisk (*) indicates that the pore size distribution shows a bi-population in the mesoporous range

	Calcination temp. (°C)	$D(V_{meso}/2)$ (nm)	V_{meso} (mL/g)	V_{macro} (mL/g)	V at $P/P_{0\ max}$ (g/mL)	Surface BET (m^2/g)
Pural SB3 Conv	700	10,37±0,21	0,66±0,03	0,01±0	0,743±0,015	225±11,25
Powder X Conv	540	11,15±0,22	0,77±0,04	0,02±0	-	262±13,1

Annex 4 – Toluene conversion

The toluene conversion obtained in the catalytic testing of Catalyst Set 1 group samples that was used to calculate the intrinsic toluene HYD rate is presented in Table iv.

Table iv - Toluene conversion obtained in the catalytic test

	Toluene conversion (%)
Mo_7+Pural SB3 Conv	0,75
MoP+Pural SB3 Conv	1,02
Mo_7+Powder X Conv	0,45
MoP+Powder X Conv	0,55
Mo_7/Powder X Conv	1,92

Annex 5 – FX results and conversion to metal loading

The FX results are presented in Table v. These values were taken as indicative since the method used was a semi quantitative one with a large error associated.

Table v – FX results for Catalyst Set 1

	Al %(w/w)	Mo %(w/w)	P %(w/w)	**MoO_3** %(w/w_{cata})	**P_2O_5** %(w/w_{cata})
Mo_7+Pural SB3 Conv	38,0	3,7	-	7,1	-
MoP+Pural SB3 Conv	36,0	4,9	0,7	9,6	2,1
Mo_7+Powder X Conv	36,0	5,0	-	9,8	-
MoP+Powder X Conv	33,0	4,8	0,7	10,2	2,1

The calculation of the metal loading from the FX results is exemplified by the case of MoP+Pural SB3 Conv in Table vi. The metal loading is given on the basis of the weight of the catalyst defined as the sum of the oxide species that would be present after calcination.

For 100g of analysed product, the mass of oxide species that would be present after calcination is calculated.

Table vi –Example of metal loading calculation

	FX results				
	g/100g	mol Al	mol Al_2O_3	g Al_2O_3	
Al	36	1,33	0,67	68,02	
		mol Mo	mol MoO_3	g MoO_3	**MoO_3 %(w/w_{cata})**
Mo	4,9	0,05	0,05	7,35	9,6%
		mol P	mol P_2O_5	g P_2O_5	**P_2O_5 %(w/w_{cata})**
P	0,7	0,02	0,01	1,60	2,1%
			Total (g_{cata})	77,98	

Annex 6 – Intrinsic toluene HYD rate error propagation

The error of the intrinsic toluene HYD rate was calculated considering that the toluene conversion has a relative error of ±10% and the PD as a relative error of ±3%. This calculation will be exemplified for the catalyst Mo7+Pural SB3 Conv:

$$\sigma_{mass\ MoO_3} = \frac{10}{100} * \frac{100 - 22{,}85}{100} * 0{,}45 * (0{,}03 * 0{,}823) = cte * \sigma_{PD} = 8{,}57 * 10^{-4}\ g$$

$$\sigma_{atoms\ Mo} = \frac{6{,}023 * 10^{23}}{143{,}94} * 8{,}57 * 10^{-4} = cte * \sigma_{mass\ MoO_3} = 3{,}59 * 10^{18}$$

$$\sigma_{\frac{1}{atoms\ Mo}} = \frac{1}{1{,}20 * 10^{20}} * \frac{3{,}59 * 10^{18}}{1{,}20 * 10^{20}} = \frac{1}{atoms\ Mo} * \frac{\sigma_{atoms\ Mo}}{atoms\ Mo} = 2{,}51 * 10^{-22}$$

$$\sigma_{\frac{toluene\ feed\ moleules}{h} * \frac{1}{atoms\ Mo}} = 9{,}35 * 10^{20} * 2{,}51 * 10^{-22} = cte * \sigma_{\frac{1}{atoms\ Mo}} = 0{,}235$$

$$\sigma_{vHYD} = 0{,}0587 * \sqrt{\left(\frac{0{,}1 * 0{,}750}{0{,}750}\right)^2 + \left(\frac{0{,}235}{9{,}35 * 10^{20} / 1{,}20 * 10^{20}}\right)^2}$$

$$= vHYD * \sqrt{\left(\frac{\sigma_{\%HYD\ converted\ toluene}}{\%HYD_{\ converted\ toluene}}\right)^2 + \left(\frac{\sigma_{\frac{toluene\ feed\ moleules}{h} * \frac{1}{atoms\ Mo}}}{\frac{toluene\ feed\ moleules}{h} * \frac{1}{atoms\ Mo}}\right)^2}$$

$$= 0{,}006\ toluene \frac{molecules}{Mo} atom/h$$

Annex 7 – XRD results

The diagrams obtained in XRD analysis are presented in Figure i.

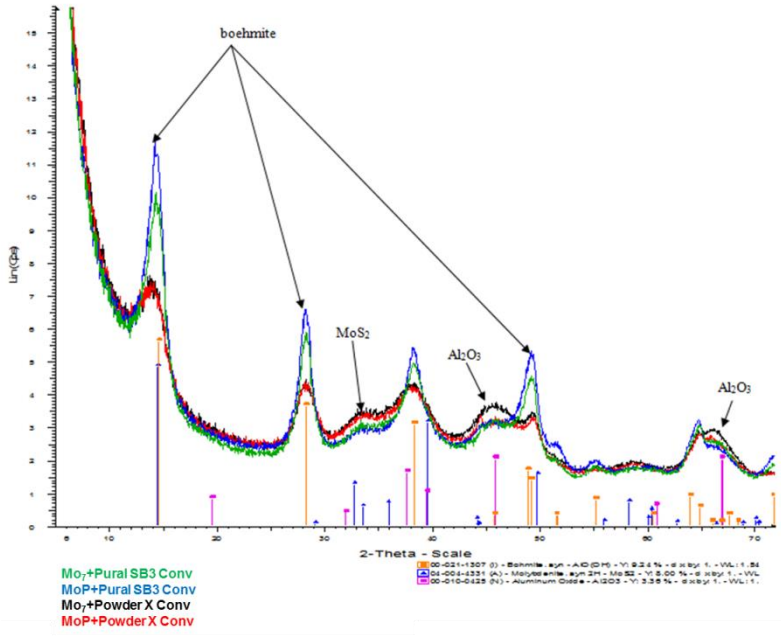

Figure i –XRD diagrams of Catalyst Set 1 products